



## Impactites of the Yaxcopoil-1 drilling site, Chicxulub impact structure: Petrography, geochemistry, and depositional environment

Burkhard O. DRESSLER,<sup>1, †\*</sup> Virgil L. SHARPTON,<sup>2</sup> Craig S. SCHWANDT,<sup>3</sup> and Doreen AMES<sup>4</sup>

<sup>1</sup>Lunar and Planetary Institute, 3600 Bay Area Boulevard, Houston, Texas 77058, USA

<sup>2</sup>Geophysical Institute, University of Alaska, Fairbanks, Alaska 99709, USA

<sup>3</sup>Lockheed Martin, 2400 Nasa Road 1, C23, Houston, Texas 77058, USA

<sup>4</sup>Geological Survey of Canada, Ottawa, K1A 0E8, Canada

<sup>†</sup>Present address: 185 Romfield Circuit, Thornhill, Ontario, L3T 3H7, Canada

\*Corresponding author. E-mail: [burkhard@allstream.net](mailto:burkhard@allstream.net)

(Received 6 October 2003; revision accepted 12 May 2004)

---

**Abstract**—The impact breccias encountered in drill hole Yaxcopoil-1 (Yax-1) in the Chicxulub impact structure have been subdivided into six units. The two uppermost units are redeposited suevite and suevite, and together are only 28 m thick. The two units below are interpreted as a ground surge deposit similar to a pyroclastic flow in a volcanic regime with a fine-grained top (unit 3; 23 m thick; nuée ardente) and a coarse breccia (unit 4; ~15 m thick) below. As such, they consist of a mélange of clastic matrix breccia and melt breccia. The pyroclastic ground surge deposit and the two units 5 and 6 below are related to the ejecta curtain. Unit 5 (~24 m thick) is a silicate impact melt breccia, whereas unit 6 (10 m thick) is largely a carbonate melt breccia with some clastic-matrix components. Unit 5 and 6 reflect an overturning of the target stratigraphy. The suevites of units 1 and 2 were deposited after emplacement of the ejecta curtain debris. Reaction of the super-heated breccias with seawater led to explosive activity similar to phreomagmatic steam explosion in volcanic regimes. This activity caused further brecciation of melt and melt fragments. The fallback suevite deposit of units 1 and 2 is much thinner than suevite deposits at larger distances from the center of the impact structure than the 60 km of the Yax-1 drill site. This is evidence that the fallback suevite deposit (units 1 and 2) originally was much thicker. Unit 1 exhibits sedimentological features suggestive of suevite redeposition. Erosion possibly has occurred right after the K/T impact due to seawater backsurge, but erosion processes spanning thousands of years may also have been active. Therefore, the top of the 100 m thick impactite sequence at Yaxcopoil, in our opinion, is not the K/T boundary.

---

### INTRODUCTION

The drilling project at the Hacienda Yaxcopoil, approximately 40 km southwest of Mérida, Yucatán, has been completed as part of the Chicxulub Scientific Drilling Project during the winter months of 2001/2002. The drill site Yaxcopoil-1 (Yax-1) is located about 60 km from the center of the impact structure (Fig. 1), in the outer part of an annular trough, or, more likely, at the rim of the excavation cavity. It was selected based on the projection of offshore seismic profiles (Cristeson et al. 1999; Snyder and Hobbs 1999) and interpreted to lie beneath approximately 800 m of Tertiary limestone, probably still within a 60 to 70 km radius transient cavity (Urrutia-Fucugauchi et al. 2001). Based on the results of the Y6 PEMEX (Petróleos Mexicanos, company files; Sharpton et al. 1996) petroleum exploration well, located

about 20 km from Yax-1, beneath the Tertiary cover rocks, project organizers expected several hundred meters of fallback suevite to overlie a coherent impact melt sheet that had been encountered at a depth of ~1295 m to the final depth of 1645 m at the Y6 site. The historic geophysical surveys by PEMEX and pre-drilling, regional geophysical investigations and interpretations (i.e., Christeson et al. 1999; Brittan et al. 1999; Hildebrand et al. 1995; Marin et al. 2000; Morgan and Warner 1999; Snyder and Hobbs 1999; Sharpton et al. 1993, 1996) were fundamental in the selection of the Yaxcopoil location.

The prediction of the project geophysicists (Urrutia-Fucugauchi 2001) appeared to be correct when the drill encountered impact breccias at a depth of ~795 m beneath Tertiary limestones, minor chert, and conglomeratic calcareous mass flows. However, after drilling through only

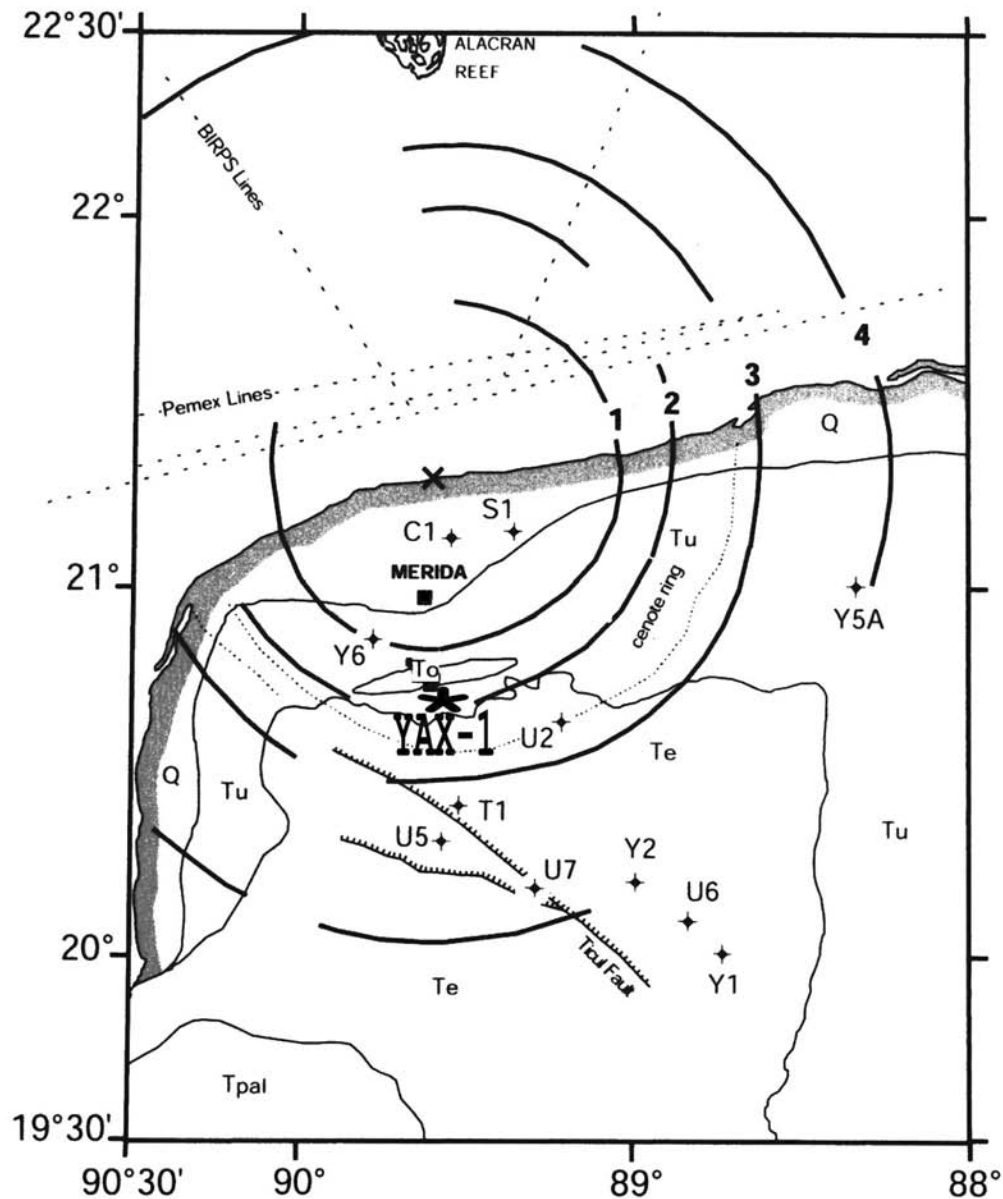


Fig. 1. The Chicxulub impact structure in Yucatán, Mexico, showing the location of well Yax-1, surface geology, assumed location of rings from gravity surveys, and some other well sites. Carbonate units at surface: Q = Quaternary; Tu = upper Tertiary; To = Oligocene; Te = Eocene; and Tpal = Paleocene. Hatched line: Ticul Fault. Dashed lines: zones of ceotes or sinkholes. Also shown are PEMEX and BIRPS offshore seismic lines. After Marin et al. (2000).

100 m of various impact breccias and melt rock, the drill encountered Cretaceous limestones, dolomite, and anhydrite cut by various minor impact breccia dikes. Dips of the Cretaceous rocks range from 0 to about 60 degrees, and the distribution of dips and their abrupt change at several locations down-hole suggest that the Cretaceous rocks make up several large megablocks. Several, up to 45 m thick, authigenic dolomite breccia zones occur beneath 1298 m (Dressler and Reimold Forthcoming). The final depth was reached at 1511 m (unpublished preliminary stratigraphy of Yax-1, Dressler 2002; Dressler et al. 2003).

The objective of this investigation is to come to an

understanding of the depositional impact environment that was active at location Yax-1. Hopefully, in a future publication, this will allow us to integrate our results and interpretations with what is known from geophysics and other drill sites within and around the Chicxulub impact structure.

In the following, we focus on the 100 m thick impactite sequence (795–895 m), which was subdivided by one of us (B. O. Dressler) at the drill site into 6 units, as shown in Table 1. We applied standard petrographic, microprobe, scanning electron microscope (SEM), and geochemical methods to characterize the various breccias and melt rocks, beginning with the units just beneath the Tertiary cover rocks.



Fig. 2. Two core samples of unit 1: a) the transition of laminated Tertiary limestone interlaminated with thin suevitic material and laminated, redeposited suevite below; b) clast-size sorted suevite. Cores have a diameter of 64 mm.

The Yax-1 impact breccias and melt rocks make up a complex sequence of rocks. To our knowledge, similar sequences are not exposed at any other terrestrial impact structure. The Yax-1 depositional environment, however, is probably not unique. Similar rock sequences may be present at other locations in the Chicxulub structure and, possibly, at other terrestrial impact structures. Elsewhere, they apparently did not survive erosion. For example, at the other two very large terrestrial impact structures, the >200 km in diameter Sudbury structure in Canada (Dressler 1984; Grieve et al. 1991; and references therein) and the >250 km in diameter Vredefort structure in South Africa (Reimold and Gibson 1996, and references therein).

Our investigations are based on B. Dressler's work of on-site scientist at the Yax-1 drill site in Yucatán, on detailed macroscopic and microscopic petrography, and on microprobe and SEM research on approximately 60 polished standard-size thin sections distributed evenly over the identified impactite units. Analytical methods are described in an appendix at the end of this paper. The small size of the Chicxulub core samples make investigation and interpretation of Yax-1 breccias difficult, if not impossible, in places. We are, however, confident, that our work, in combination with that of others in this special publication and elsewhere, will eventually lead to a solid understanding of the Yax-1 depositional environment, which, in turn, will enhance our knowledge of large scale impact processes and the effects they can have on the environment and life on Earth.

## PETROGRAPHY

### Introduction

We applied standard macroscopic and light microscope methods to characterize the groundmass of breccias and melt rocks, and the types, size and shapes of fragments. Sixty five polished thin sections, with approximately an equal number for each of the six rock units, were studied under the light microscope and under SEM and microprobe at the NASA Johnson Space Center, Houston, Texas (for instrumental parameters, please see Appendix). The proper characterization of breccia matrices is paramount in the interpretation of the origin of the breccia. Clastic-matrix groundmasses and melt matrices were identified. While the character of the matrix of some of the six impactite units is homogeneous melt or clastic, in other units, matrices apparently are clastic in one small sample and melt in others.

### Unit 1

In the drill log (Table 1), unit 1 was named "redeposited suevite." The unit has a thickness of 13.39 m and, as all the drill cores of Yax-1, has been logged at the drill site by B. Dressler (Table 1, unpublished logs and Dressler et al. 2003). In Fig. 2, two core samples of it are shown. The upper core represents the laminated transition zone between Tertiary limestone and redeposited suevite where fine calcarenite is

Table 1. Log and preliminary petrography of well Yax-1, Chicxulub impact structure.

Depth (m)	Thickness (m)	Log name	Petrography	Breccia unit
Tertiary (cover rocks)				
0.00–794.63	794.63	Sedimentary rocks	Massive, laminated, and crosslaminated calcarenite, calcareous siltstone; minor chert. Soft-sediment deformation features, bioturbations, planktic foraminifers. Beneath 600 m, several conglomeratic mass flows.	
794.63–808.02	13.39	Redeposited suevite	Melt-rich, average clast size <0.5 cm. Overall very good clast size sorting. Laminated on top 1.60 m. In places, weak horizontal alignment of elongate clasts. Clasts of target rocks and melts of various colors. Largest clast 4.0 cm. Contact with overlying limestone is gradational over about 20 cm, contact with unit 2 abrupt. Carbonaceous, greenish-grey groundmass.	1
808.02–822.86	14.86	Suevite	Melt-rich, coarser-grained than unit 1. Carbonaceous, greenish grey groundmass. Clasts: Basement rocks (max. size 6.4 cm), sedimentary rocks (max. size 3.5 cm), melt (various colors, max. size 9.0 cm). Contact with unit 3 is abrupt.	2
822.86–845.80	22.94	Chocolate brown melt breccia	Chocolate-brown when wet, greyish when dry. Groundmass is very fine-grained to aphanitic. Some melt fragments exhibit long, schlieren-like shapes suggestive of flow. Relatively few large clasts: Basement rocks (max. size 18 cm) sedimentary rocks (max. size 3.5 cm), melt (max. size 26 cm). Contact with unit 4 is gradational.	3
Impact breccias and melt rocks				
845.80–861.06	15.26	Variegated, glass-rich suevitic breccia	Groundmass is similar to that of unit 3. Wide variety of laminated and unlaminated melts of various color, shapes, and sizes. Shapes are suggestive of flow and ductile and brittle deformation. Scarce welding features. Clasts: Basement rocks (max. size 16 cm, sedimentary rocks (max. size 4 cm, melt (various colors, max. size 22 cm). Contact with unit 5 is abrupt.	4
861.06–884.92	23.86	Green, monomictautogene melt breccia	Mainly green melt fragments in an arrangement similar to rhyolite fragments in a rhyolite flow top breccia. Lamination in neighboring clasts, in places, show continuous orientation. Inclusions are relatively scarce but, in places, large: Basement rocks (max. size 6.4 cm), sedimentary rocks (max. size 40 cm). Green melt fragments have a max. size of 15 cm. Shapes of basement rock inclusions commonly suggestive of incipient melting. Contact with unit 6 is gradational/abrupt.	5
884.92–894.94	10.02	Variegated polymict, allogenic clast melt breccia	Rich in melt fragments that are commonly laminated and have various colors. They have contorted shapes, shard-like shapes, and, in places, exhibit shapes suggestive of welding. Green fragments as in unit 5 are present but commonly take on a “bleached” tan color. Carbonate melt fragments and, at the bottom of unit 6, carbonate melt with inclusions of target rocks and melt. Clasts: Basement rocks (max. size 34 cm), sedimentary rocks (Max. size 53 cm), and melt (max. size 20 cm)	6
Cretaceous (megablocks)				
894.94–1510.97	616.03	Limestone, dolomite, anhydrite. Impact breccias	Sedimentary rocks are fine-grained to very fine-grained, massive to bedded. Sedimentary features observed: lamination, wavy lamination, soft sediment deformations, scarce intraclasts. Impactites: melt dike, polymict, clastic-matrix breccia dikes, several dolomite autoclastic breccia bodies up to 45 m thick. Variable inclination of bedding planes, suggestive of the presence of several megablocks. Anhydrite makes up 27.4% of the rocks beneath unit 6 impactites.	

interlaminated with fine reworked suevitic rock. The lower core is not laminated but is relatively fine-grained (Table 1), size-sorted, and rarely exhibits horizontal alignment of tiny elongate clasts. Lamination of this rock unit is present only in the uppermost 1.6 m.

No thin sections of the upper-most impactite unit were investigated and no chemical work was performed on samples of unit 1. Macroscopic observation of an approximately 1.6 m

thick zone of laminated breccia at the very top of the unit, the overall very small clast size, and, in places, a faint horizontal alignment of tiny elongate clasts, differentiates this unit from the five impactite units below. Basement rock fragments are granite, granodiorite, and gneiss. Limestone and very scarce chert clasts occur. Melt fragments are ubiquitous and are black, brown, or greenish-grey in color. (We use the term “melt” for various types of fresh or altered, microlite-bearing

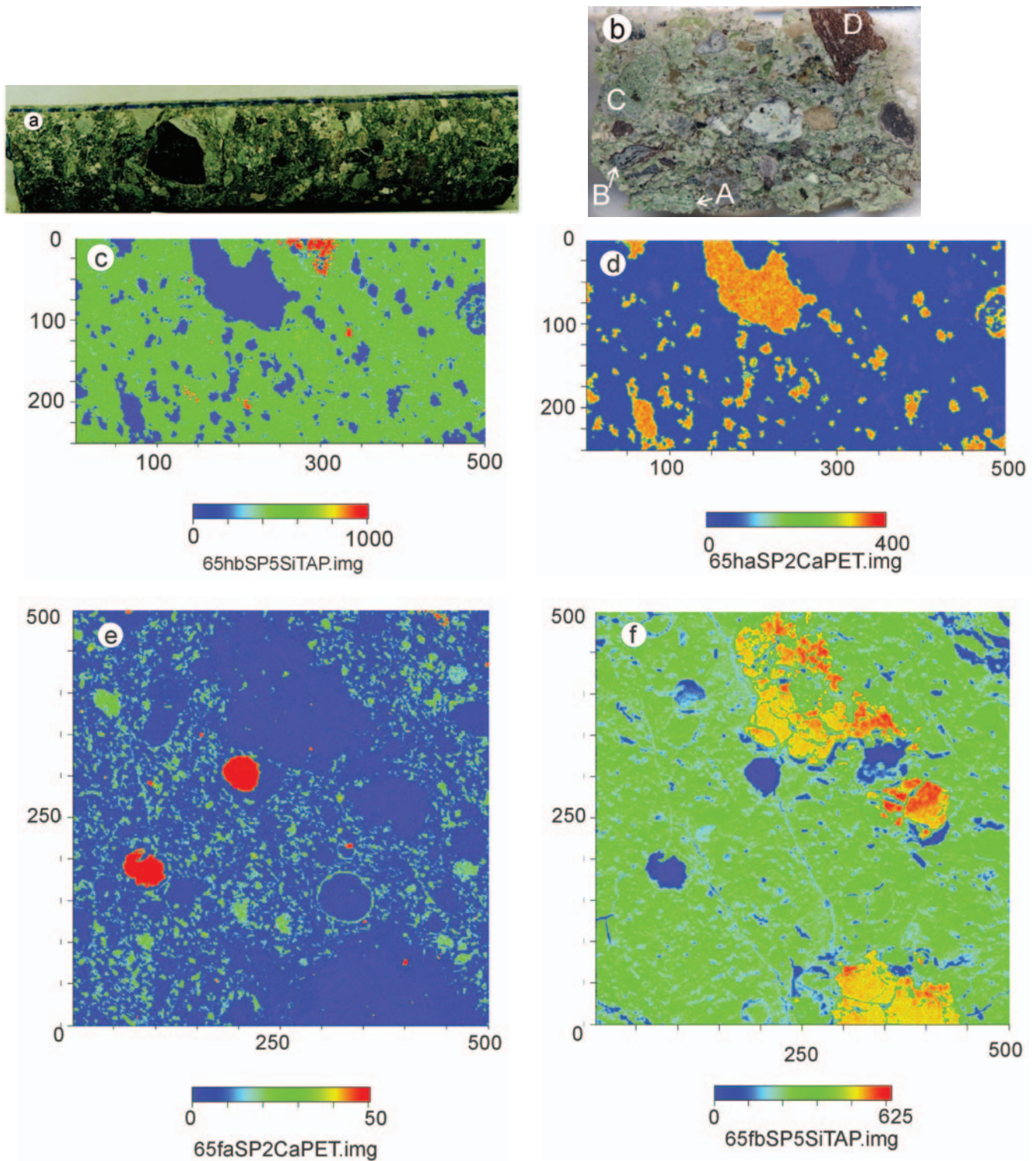


Fig. 3. Petrography of unit 2 (log name "suevite") at various scales: a) core sample with clasts of various sizes and shapes. The large, dark angular to subrounded fragment is partially cored. Most light grey clasts are limestone, most greenish clasts altered melt. Core has a diameter of 64 mm; b) scan of a 4 cm long, thin section (Yax-1-819.65). Almost all recognizable clasts are melts. Clasts A and B were analyzed for major element composition (see section Geochemistry). Element maps: Si of (c) and Ca of (d) are from clast D; Ca of (e) and Si of (f) are from clast C, of scanned thin section (b). Note the various shapes and colors of the melt fragments, some of which are laminated, some are not. The shape of the calcite areas in the element maps of (c) and (d) are suggestive of immiscible carbonate melt in silicate melt. Calcite in (e) and (f) may represent amygdules. The dimensions of (c-f) are in  $\mu\text{m}$ . (The sample number designates the depth of core from which the specimen was obtained.)

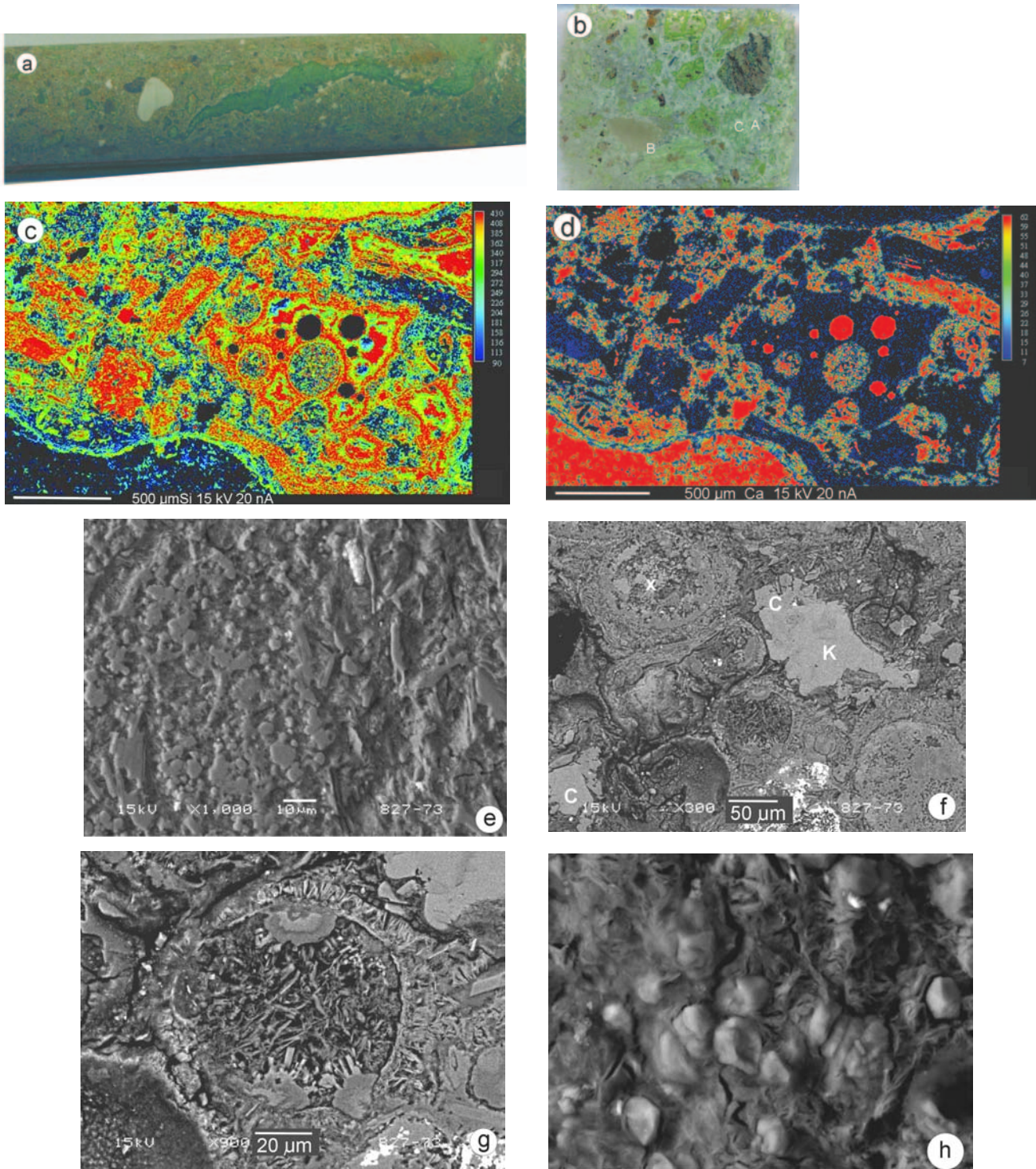


Fig. 4. Petrography of unit 3 (log name “chocolate-brown melt breccia”) at various scales: a) core sample with long, schlieren-like green melt body and a light grey limestone clast in very fine-grained brownish groundmass. The core diameter is 64 mm; b) scan of a 4 cm-long thin section (Yax-1-827.73). Various melt fragments in very fine-grained groundmass. A = the approximate location of (c) and (d); B = the approximate location of (e); C = the approximate location of (f) and (g); c) Si-element map of frothy, amygdaloidal melt or immiscible melt; d) Ca-element map with melt as (c); e) groundmass at location B of thin section scan. It consists of irregular, grain-like bodies of carbonate in smectite and some lath-shaped alkali feldspar; f) chondrule-like bodies: upper body left has calcite and smectite centers rimmed by plagioclase. The dumbbell-shaped body beneath consists of calcite and smectite. The spherical body below the center of the image, also shown in (g), consists mainly of smectite with some minor alkali feldspar near its rim. The sphere at the lower right corner of the image consists mainly of alkali feldspar with minor smectite and calcite; g) enlargement of one of the “chondrules” of (f); h) Yax-1-832.21 depicts groundmass consisting of subangular grains of grey calcite and very scarce wollastonite in dark grey smectite (saponite). The length of this image is 42 mm.

or microlite-free “glass” and melt fragments). The very fine-grained groundmass is clastic and commonly carbonaceous.

The lower contact of this unit with unit 2 is not very well defined. M. Rebolledo-Vieyra (personal communication; Instituto de Geofísica, UNAM, Mexico City) did not notice an apparent difference between the paleomagnetic signatures of the two suevite units (unit 1 and unit 2). However, further investigations in minute detail at the boundary of the two units are recommended and may show slightly different paleomagnetic signatures.

## Unit 2

The suevite of unit 2 (thickness 14.86 m; log name “suevite,” Table 1) is characterized by considerably coarser clast sizes than that of the unit above and by the absence of any sedimentary features indicative of reworking or redeposition. Maximum clast sizes are larger than in unit 1, but clast types are more or less the same, namely granite, gneiss, limestone, dolomite, and brown, greenish and black melt. The groundmass is fine-grained and commonly carbonaceous. Compared to suevite from some other terrestrial impact craters, the unit 2 suevite is very rich in melt fragments.

Figure 3 provides petrographic images at various scales, from drill core to electron microprobe, and some explanation in the figure caption. The melt fragments investigated contain tiny inclusions of quartz and calcite, the latter based on their shapes, probably representing amygdules and immiscible melt. In the thin section scan of Fig. 3b, the melt fragments investigated in detail are marked. Laminated and non-laminated melt fragments occur. Note the truncation of the lamination by the border of some of the fragments. Tiny microlites in the melt fragments were chemically identified as pyroxene and potassium feldspar.

The clastic groundmass (material <1–3 mm in size) of unit 2 consists of tiny melt, mineral and rock fragments. No melt fragment shapes indicative of welding were observed.

## Unit 3

Unit 3 (log name “chocolate-brown melt breccia,” thickness 22.94 m; Table 1) is probably the most enigmatic rock type encountered at Yax-1. When fresh out of the drill hole, the very fine-grained to aphanitic groundmass of the rock has a chocolate-brown color and becomes brownish-grey when dry. Clasts are up to 26 cm in core length. Some large, green melt fragments exhibit schlieren-like shapes suggestive of flow, in part parallel to the core axis (Fig. 4a). The fine groundmass makes up 60–95 vol% of the rock. Sedimentary rock clasts are limestone, possibly also some dolomite. No anhydrite was observed. In general, basement rock clasts are scarce. Granite and gneiss are the most common rock fragments derived from the basement. Granite clasts are up to

18 cm in core length, but most clasts are smaller. Gneiss is the second most common type, with a maximum size of 6 cm. Aplite is scarce, as are biotite schist and gabbro. The latter type measured up to 11 cm. The very fine-grained, strongly hematized biotite schist was initially wrongly identified as amphibolite in the well log (Table 1). An image of a thin section of unit 3 is shown in Fig. 4b.

Under the petrographic microscope, the groundmass consists of tiny, altered greenish melt fragments and very fine-grained carbonate. The melt fragments have angular, shard-like, round-globular, to elongate lensoid shapes. Internal textures are difficult to recognize. Most are indistinct, but some tiny clasts have flow textures that are truncated by the boundary of the fragments, an observation also made on larger melt fragments. This observation suggests that at least some of the shards (e.g., Yax-1-826.06) are derived from larger laminated melt bodies. In many places, the tiny melt clasts are rimmed by iron oxide, probably hematite, which is responsible for the brownish color of the rock. While in some thin sections of unit 3, finest-grained carbonate appears to fill the space between the tiny melt fragments, in others (e.g. Yax-1-826.06, 839.34, and 842.06) all the groundmass consists of a dense mass of even smaller, altered melt fragments, with very minor carbonate. In Yax-1-826.06 and elsewhere, some of the tiny melt fragments exhibit welding features. Only a few centimeters below in the core, in another thin section, the groundmass is very carbonate-rich.

In Yax-1-827.73, we observed a texture that is possibly indicative of the presence of immiscible silicate-carbonate melt. It consists of a frothy, green altered melt with amygdule-like bodies rich in very fine-grained carbonate (Fig. 4c), in texture identical to the carbonate in the groundmass of this rock. These amygdule-like bodies are large in comparison with the very thin bubble walls. Some smaller “amygdules” consist solely of calcite. The thin walls are commonly broken and tiny shards—fragments of the walls—lie embedded in the carbonate close to the foamy melt fragment. In Yax-1-839.34, a similar, “amygdaloidal” melt with somewhat thicker walls has large, oval, carbonate filled “amygdules.” Where the melt is broken and an “amygdule” is open against the groundmass, one can easily compare the very fine-grained “amygdule” carbonate with the very fine-grained groundmass carbonate. There is no difference. The carbonate in the “amygdules” cannot be clastic carbonate. It has to represent an alteration product or, more likely, a melt.

Also in Yax-1-827.73, we have observed numerous spherical and dumbbell-like bodies that resemble bodies interpreted by Graup (1981) as chondrules in suevite of the Ries impact crater. Figure 4f depicts several of these bodies. Compositionally they are very heterogeneous, as described in the caption of this figure. “Chondrules” consisting of tiny shard-like melt fragments, tiny feldspar laths, and smectite also occur. In places, “chondrules” are embedded in melt that consists of smectite, calcite and alkali feldspar that wraps

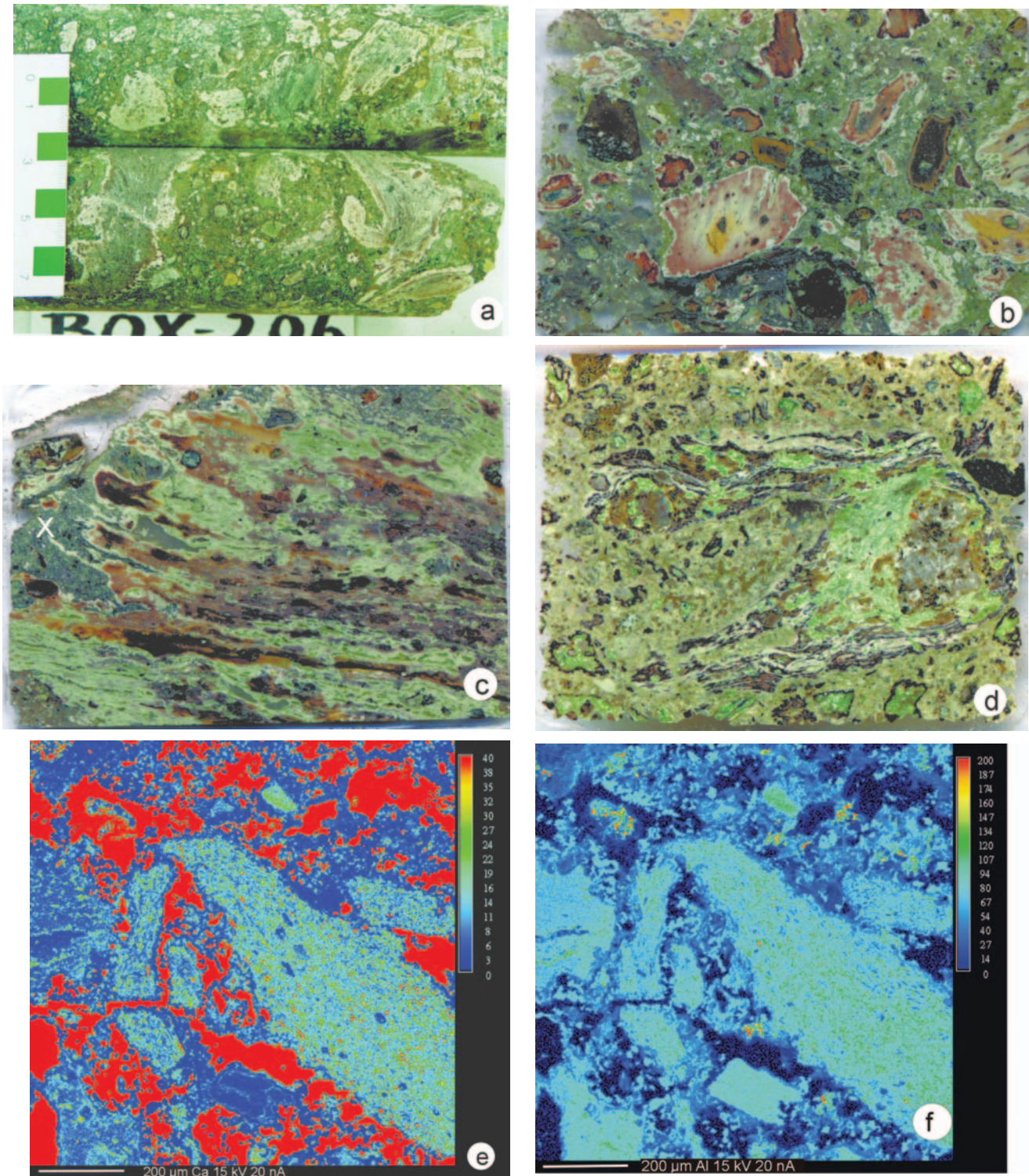


Fig. 5. Petrography of unit 4 (log name “variegated, glass-rich suevitic breccia”) at various scales: a) core samples with commonly laminated, in places contorted melt fragments in very fine-grained groundmass; b) scan of 4 cm long thin section (Yax-1-859.42). Various melt fragments in very fine-grained groundmass; c) scan of 4 cm long thin section. One large laminated melt fragment with melt/groundmass interfingering at location x (sample 857.78); d) scan of 4 cm long thin section. A large, U-shaped, laminated melt fragment. Shape of fragment is indicative of absorption of melt by groundmass; e) Ca-element map of interfingering of melt with groundmass at location x of (c). Note the bending of melt fragment tongue and melt relicts in calcite/silicate groundmass, which is interpreted as clast-rich carbonate/silicate melt. Calcite is red. f) Al-element map of same location as in (e) and (g).

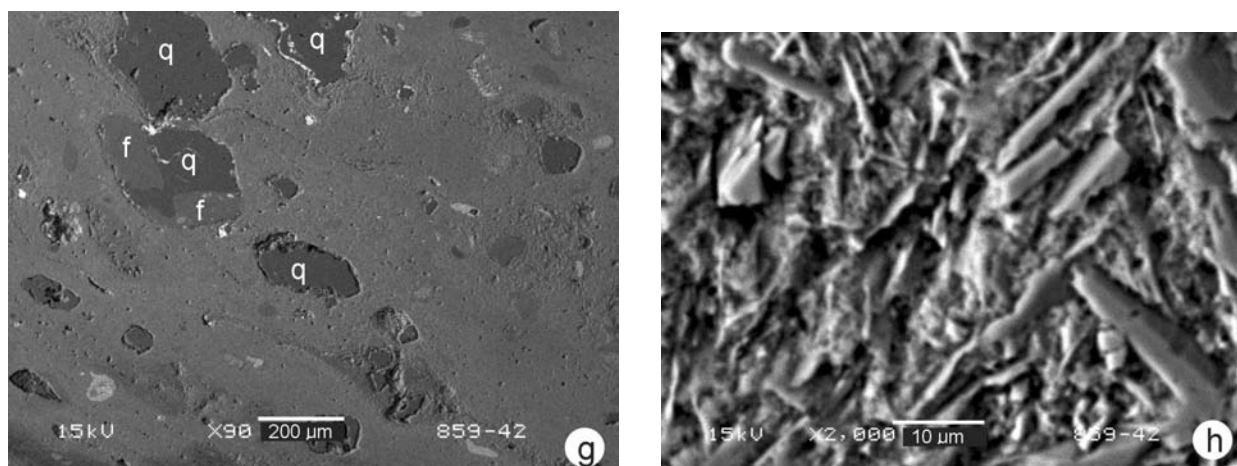


Fig. 5. *Continued.* g) melt containing quartz (q), basement rock (f+q), and plagioclase-minor alkali feldspar (f) inclusions in feldspathic melt fragment, the brown fragment with light brown rim in center of thin section of (b), just north of the largest fragment in (b); h) melt of the largest fragment of (b) consisting of plagioclase laths, minor diopside (light grey mineral) and minor smectite mesostasis.

around the “chondrules.” The chondrule-like bodies of unit 3 are distinctly different from accretionary lapillis that have been observed in suevitic rocks of the Sudbury structure (W. V. Peredery, INCO Limited, personal communication, 1983), the Wanapitei Structure (B. O. Dressler, unpublished data), and the Ries structure (Graup 1981). The large green, in places schlieren-like, melt inclusions (Fig. 4a) commonly have flow lamination and tiny, flow-aligned inclusions. Amygdules, where observed, contain carbonate rimmed by smectite, or smectite alone. In Yax-1-842.06, green melt clasts have tiny plagioclase microlites that are flow-aligned. Amygdules in this sample contain carbonate and are flow-aligned or contain radiating actinolite. Carbonate “amygdules” may represent an immiscible melt. Dark grey, almost black, and brown melt fragments also occur in unit 3 impactite but are not common.

#### Unit 4

Unit 4 (log name “variegated, glass-rich suevitic breccia,” thickness 15.26 m; Table 1) is an impact breccia characterized by a wide variety of melt fragments. The clasts are commonly laminated and have contorted shapes, shard-like shapes, and exhibit features indicative of ductile and brittle deformation. The lamination of some clasts is truncated by the border of the fragments, whereas at other clasts, the lamination is parallel to the contorted shape of the fragment. Welding between some melt fragments has occurred. In contrast to the rocks of unit 3 above, macroscopic melt clasts are plentiful and, in places, densely packed. Basement rock fragments (maximum size 16 cm) are granite, various types of gneiss, garnet amphibolite, diorite, and granodiorite (macroscopic classification is based on color index only). Limestone (max. size 4 cm) and minor dolomite, but again no anhydrite clasts have been observed. Melt fragments (max. size 22 cm) are green, black, or brown.

Under the light- and electron microscope, the groundmass resembles that of unit 3 above. However, in places, it has features indicative of a melt, which has reacted with small melt bodies. Matrix melt and melt body are partially interfingered. In Fig. 5, these features are depicted, among other petrographic characteristics of unit 4, and described in the figure captions. Because of the groundmass similarities and the gradational contact with unit 3, units 3 and 4 possibly represent one depositional process. The contact with unit 5 below is quite abrupt.

#### Unit 5

Unit 5 (log name “green, monomict-autogene melt breccia,” thickness 23.86 m; Table 1) is relatively homogeneous and consists mainly of green, commonly laminated melt fragments. In the well log, it has been described as an impact melt breccia that contains angular melt fragments (max. size 15 cm) that, in places, can be put together, similar to pieces of a jigsaw puzzle. Lamination in neighboring pieces may show lamination that is continuous. Basement rock inclusions (max. size 6.4 cm) are granite, aplite, gneiss, and granodiorite. Scarce limestone clasts occur, some of which are large (40 cm). Again, no anhydrite fragments were observed. Basement rock inclusions commonly show textures suggestive of incipient melting. The incipient melt then, in places, fills the spaces between melt fragments. The contact with unit 6 below is more or less gradational.

Under the optical microscope, the groundmass between the melt fragments is heterogeneous. In one place, it may consist of tiny melt fragments similar to the macroscopic melt fragments, in others, of melt fragments and minor calcite, or of a melt similar to the melt fragments. In Fig. 6, various petrography features are shown at various scales and described in lengthy captions.

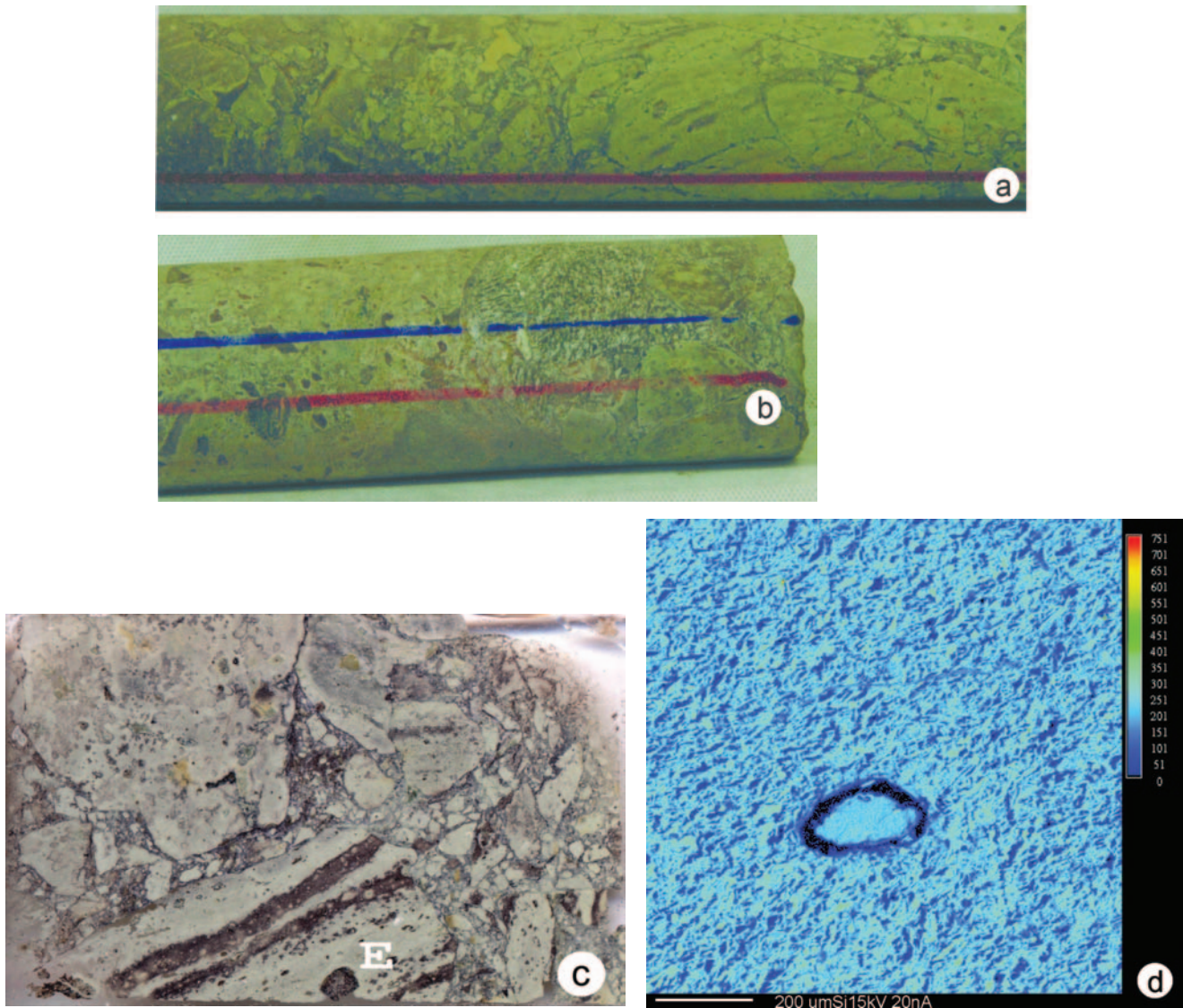


Fig. 6. Petrography of unit 5 at various scales: a) core sample showing laminated melt fragments. Core is 64 mm in diameter. Depth 871.90 m; b) core sample of green melt breccia with a gneiss inclusion with outlines indicative of incipient melting. Incipient melt in part fills spaces between melt fragments. Core is 64 mm in diameter. Depth 872.60 m; c) thin section Yax-1-864.96 showing several laminated and non-laminated melt clasts. E marks the location of BSE image and Si-element map of (d) and (e). Section is about 4 cm long; d) Si-element map of melt of thin section 864.96, see above. Inclusion consists of smectite.

### Unit 6

In the well log (Table 1), unit 6 has been described as “variegated, allogenic-clast melt breccia.” It is 10.02 m thick, very heterogeneous and contains melt fragments that are commonly laminated and have various shapes and colors. Features suggestive of welding have been observed. Melts containing inclusions of melts, e.g., black melt fragments in green melt fragments, have been noted. Similar observations have been made in UNAM 5 suevites (B. O. Dressler, unpublished report to UNAM and the International Continental Deep Drilling Program). The lower part of unit 6 is in large part a carbonate melt that contains inclusions of silicate melt fragments and various target rock fragments. At

depth 891.27, many tiny, green, and elongate silicate melt fragments are flow aligned in a carbonate melt.

Unit 6 contains the largest target rock fragments of all Yax-1 impactite breccias studied here. Basement rock clasts (max. size 34 cm) are granite, amphibolite, soapstone, ultramafic rocks, and gneisses. Limestone fragments reach 53 cm in core length, melt fragments 20 cm.

Under the microscope, the groundmass of unit 6 is heterogeneous. Melt matrix and probably clastic matrix have been noted. In Fig. 7, petrographic features of this unit are shown at various scales and briefly described in the figure captions. One microlite-bearing carbonate/silicate melt fragments was noted in carbonate melt groundmass (Figs. 7d and 7h).

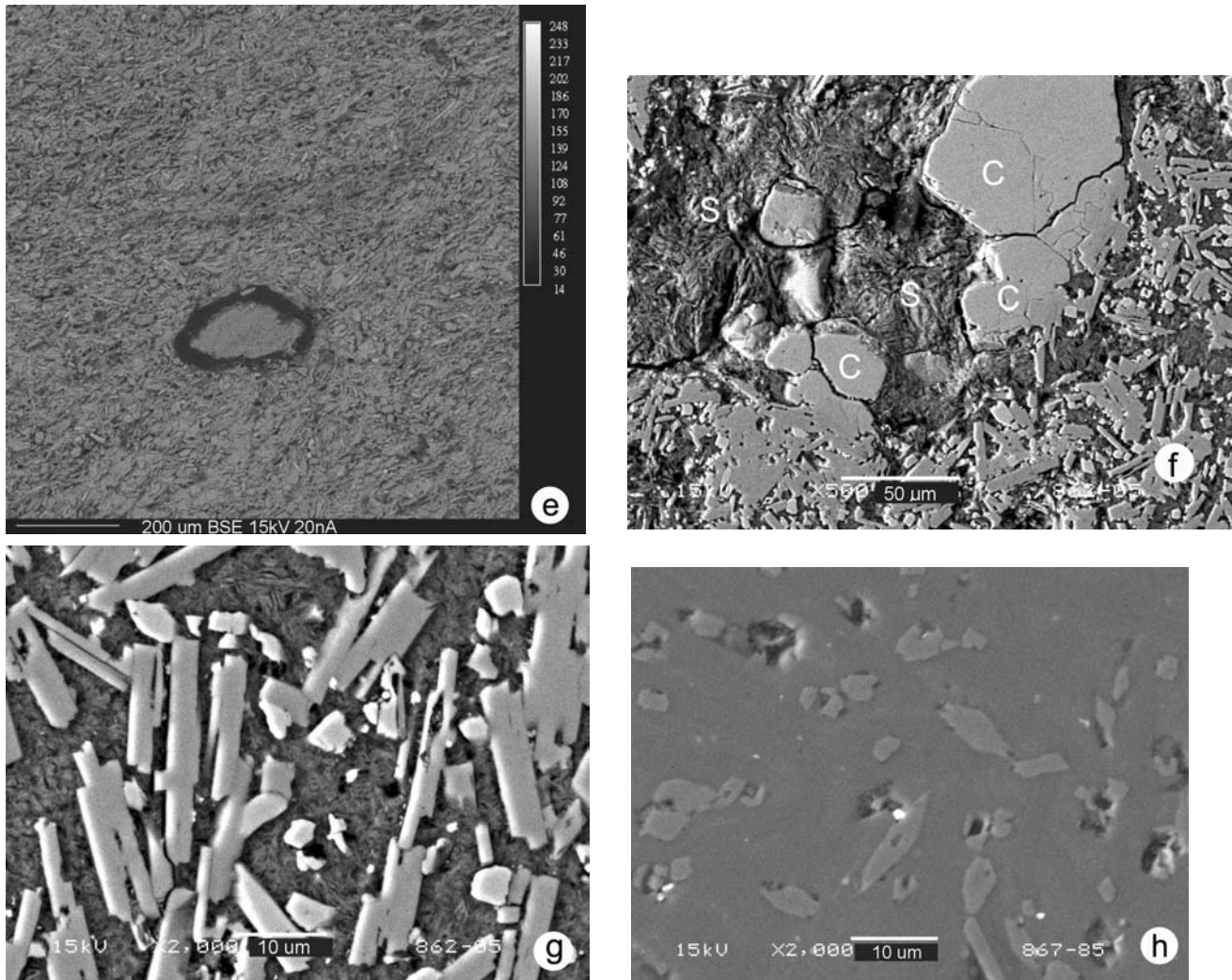


Fig. 6. *Continued.* Petrography of unit 5 at various scales: e) BSE image of melt of thin section 864.96, see above; f) groundmass between two melt fragments. Thin section Yax-1-862.05. S: smectite mesostasis; C: calcite. Long laths are plagioclase, stubby ones are diopside. Section is about 4 cm long; g) groundmass of a melt fragment in thin section Yax-1-862.05. Long, grey plagioclase laths and lighter grey, stubby diopside crystals in a smectite (saponite) mesostasis; h) diopside in an aphanitic feldspathic groundmass. Thin section Yax-1-867.85.

## GEOCHEMISTRY

The impact breccias and melt rocks of the Yax-1 well are characterized by a wide variety of target rock and melt fragments. Petrography allows determination of target rock fragments. Melt fragments represent fused target rocks or mixtures of target rocks. Their chemical compositions provide insight on the precursor lithology, on mixing processes that may have been active during melting, and on post-deposition alteration. Knowing the precursor of melt fragments in impact breccias and impact melt rocks gives the impact researcher one more clue to properly interpret the depositional environment and post-deposition alteration processes of the Yax-1 impactites.

We analyzed 24 melt fragments with a Cameca SX 100 microprobe and, semi-quantitatively, a similar number with a

JEOL scanning electron microscope. Focused beam microprobe profiles across melt fragments provide an approximate average composition of the fragment investigated and a measure on the homogeneity or heterogeneity of individual clasts, as do microprobe element maps of parts of melt fragments (Figs. 3 c–f; 4 c–d; 5 e–f; 6 g–h). In several figures (Figs. 8–15), we present representative analytical results obtained from a number of individual clasts. We selected for publication the results obtained from one or two melt fragments per impact breccia unit. A summary compilation of all microprobe profile data is shown in Table 2 and Fig. 16. No chemical data were obtained from unit 1, the redeposited suevite. In Table 2, we also compare our results with those obtained from Chicxulub wells C1 and Y6 (Schuraytz et al. 1994).

Figures 8–15 depict analytical profiles across parts of

Table 2. Chemical composition (weight %) of Yax-1 melt fragments versus depth and comparison with results from wells C1 and Y6.<sup>a</sup>

Unit	Depth	SiO <sub>2</sub>	TiO <sub>2</sub>	Al <sub>2</sub> O <sub>3</sub>	FeO	MnO	MgO	CaO	Na <sub>2</sub> O	K <sub>2</sub> O
Silicate melts										
2	819.65	61.64	0.12	18.93	4.08	0.02	1.86	2.85	1.49	9.01
	819.65	60.06	0.29	20.51	3.87	0.01	2.85	4.94	3.01	4.46
	825.15	61.23	1.50	20.49	1.70	0.02	2.14	3.75	4.06	5.11
3	825.15	61.47	1.57	18.92	2.10	0.01	1.79	3.22	3.46	7.46
	826.25	57.40	0.89	21.72	3.77	0.01	3.91	5.76	4.10	2.44
	842.06	62.89	1.08	18.97	1.48	0.01	2.55	3.35	4.10	5.57
	852.02	54.65	0.48	20.98	6.21	0.03	5.25	6.13	3.15	3.12
	852.02	59.38	0.41	19.36	2.72	0.03	2.04	7.29	4.48	4.29
4	857.78	60.55	0.58	18.82	2.72	0.03	1.64	6.42	4.29	4.95
	857.78	55.58	0.55	17.81	4.22	0.06	4.18	10.68	3.33	3.59
	857.78	53.82	0.51	16.59	4.74	0.08	5.92	12.87	3.38	2.09
	857.78	61.19	0.53	19.69	2.49	0.02	1.16	4.49	5.28	5.15
5	862.05	56.25	0.28	19.51	3.66	0.04	4.64	10.34	3.76	1.52
	864.96	51.47	0.65	20.29	9.87	0.03	4.45	7.67	4.24	1.33
	885.70	60.72	0.15	22.49	1.43	0.01	0.20	3.90	4.02	7.08
	885.70	61.47	0.51	22.01	1.03	0.12	0.16	3.05	4.05	7.60
	891.27	61.13	0.05	20.93	1.23	0.01	1.36	2.54	2.64	10.11
6	891.27	61.10	0.47	20.49	1.87	0.01	1.79	3.86	4.63	5.78
	892.32	60.49	0.92	22.39	1.08	0.01	0.72	2.39	2.76	9.24
	892.32	61.95	0.45	21.04	0.80	0.01	0.16	2.39	2.74	10.46
	894.68	62.66	0.48	19.44	1.48	0.01	0.50	2.55	2.97	9.91
	894.68	63.00	0.26	20.30	1.25	0.01	0.07	3.26	3.56	8.29
Carbonate melts										
6	885.70 <sup>b</sup>	10.83	0.02	3.44	0.29	0.38	0.15	50.60	0.66	0.64
	892.32 <sup>c</sup>	0.12						62.36		
C1		64.91	0.53	15.02	4.64	0.09	2.78	5.54	3.74	2.75
Y6 <sup>d</sup>		60.48	0.46	15.52	4.44	0.10	2.95	10.79	3.10	2.16

<sup>a</sup>Methods: Yax-1 analyses are averages of microprobe profiles across parts of melt fragments (see figures 8–15). C1 and Y6 composition of glass beads produced by direct fusion of 10 to 20 mg of powder were determined using 15 kV, 30 nA beam current and a rastered area of 20 μm × 20 μm (Schuraytz et al. 1994). All analyses presented in this table were performed at the Johnson Space Center laboratories. All analyses recalculated to 100%.

<sup>b</sup>Carbonate melt fragment.

<sup>c</sup>Carbonate melt in silicate melt fragment.

<sup>d</sup>Average of 8 published analyses.

melt fragments. They also present average profile compositions not recalculated to 100%. These averages and the results from several other profiles not shown here were recalculated to 100% and are presented in Table 2. Figure 16 is based on the recalculated Yax-1 data and shows analytical data versus depths.

Based on the relatively small number of chemical analyses (Table 2), melt fragments are relatively homogeneous. Most fragments have a silica content of between about 59 and 63 weight %. Three fragments have considerably lower SiO<sub>2</sub> of between about 51 and 55 weight %. Unit 6 differs from the other units in that it has an overall considerably higher potassium content and lower iron content. As depicted in Table 2, there are some noticeable differences between our Yax-1 results and those obtained by Schuraytz et al. (1994) from deep wells C1 and Y6 (for location see Fig. 1). The C1 and Y6 data were also recalculated by us to 100%. We are aware of the difficulties when comparing results from different laboratories.

## DISCUSSION-DEPOSITIONAL ENVIRONMENT OF YAX-1 IMPACTITES

Because of their small size, drill cores are not the best sample type for the study of coarse and heterogeneous breccias. The difficulties in properly characterizing and interpreting the various Yax-1 stratigraphic breccia units were made even more difficult by the small sample size and the small number of samples available for our study.

For this investigation, we had about 60 2 cm-thick quarter core pieces available. However, despite all these limitations, we are confident that our view of the depositional environment proposed here is a valid one.

The top 1 to 2 m of unit 1, with a log name of “redeposited suevite,” is laminated, as is the lowermost Tertiary limestone just above. The lamination and the relatively fine clast size, the clast-size sorting, and a faint horizontal alignment of tiny, elongate fragments in the breccia are evidence for reworking and redeposition of suevitic material.

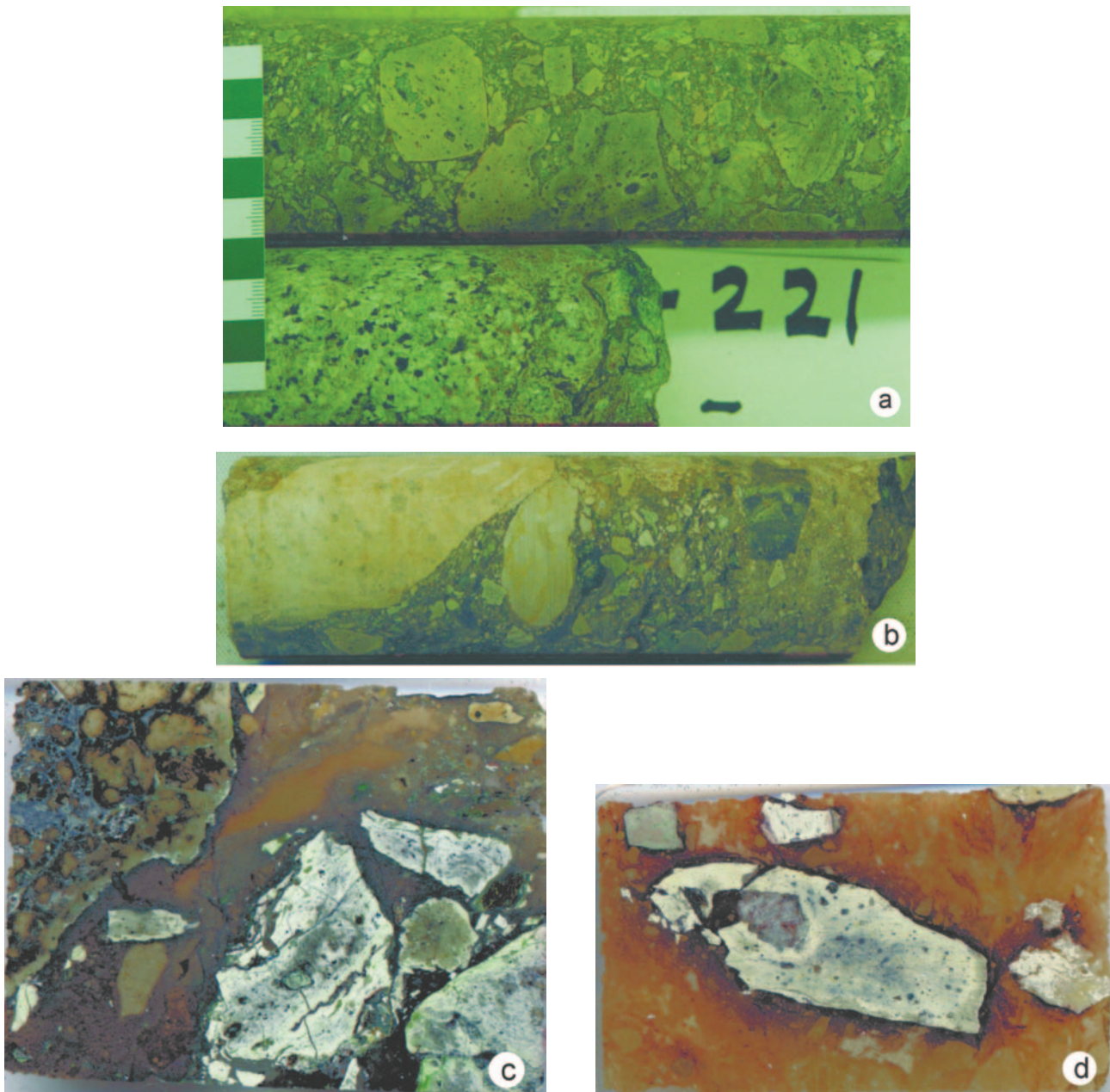


Fig. 7. Petrography of unit 6 at various scales: a) core sample showing green melt fragments that are very similar to those in unit 5. Core is 64 mm in diameter. The depth is ~889 m; b) core sample with limestone, dolomite, and melt fragments set in carbonate-rich groundmass. The core diameter is 64 mm, the depth 890.70 m; c) thin section Yax-1-892.15: “Bleached” melt fragments and tan colored, smaller carbonate rock fragments. The large fragment in upper left corner of image is a granite fragment in a stage of incipient melting. The carbonate melt groundmass has a texture suggestive of flow. The section is ~4 cm long; d) thin section Yax-1-885.70: Several grey melt fragments in a brownish carbonate groundmass that also contains somewhat lighter colored carbonate fragments that are possibly in a stage of incipient melting and incorporation into the carbonate melt groundmass. The fragment in the upper left corner of the image is a carbonate melt fragment (Fig. 7h, compare with microprobe profile of Fig. 15), the other, lighter grey fragments are silicate melt clasts.

In contrast, the “suevite” of log unit 2 has larger fragments that are relatively homogeneous in size. There is no petrographic evidence for reworking and redeposition. Therefore, we interpret unit 2 breccias as common fallback suevite.

Suevite units 1 and 2 have a total thickness of only 28 m. This is considerably less than what one would expect at a

distance of only 60 km from the center of the impact structure. At well UNAM 5, 110 km from the center, a suevite deposit at least 170 m thick underlies a 332 m thick sequence of Tertiary cover rocks. The fallback breccia at UNAM 5 (U5 in Fig. 1) also has a laminated, redeposited upper-most part, which is 15 m thick and is underlain by common suevite to the final depth of 502 m. 130 km from the center of the structure, at UNAM

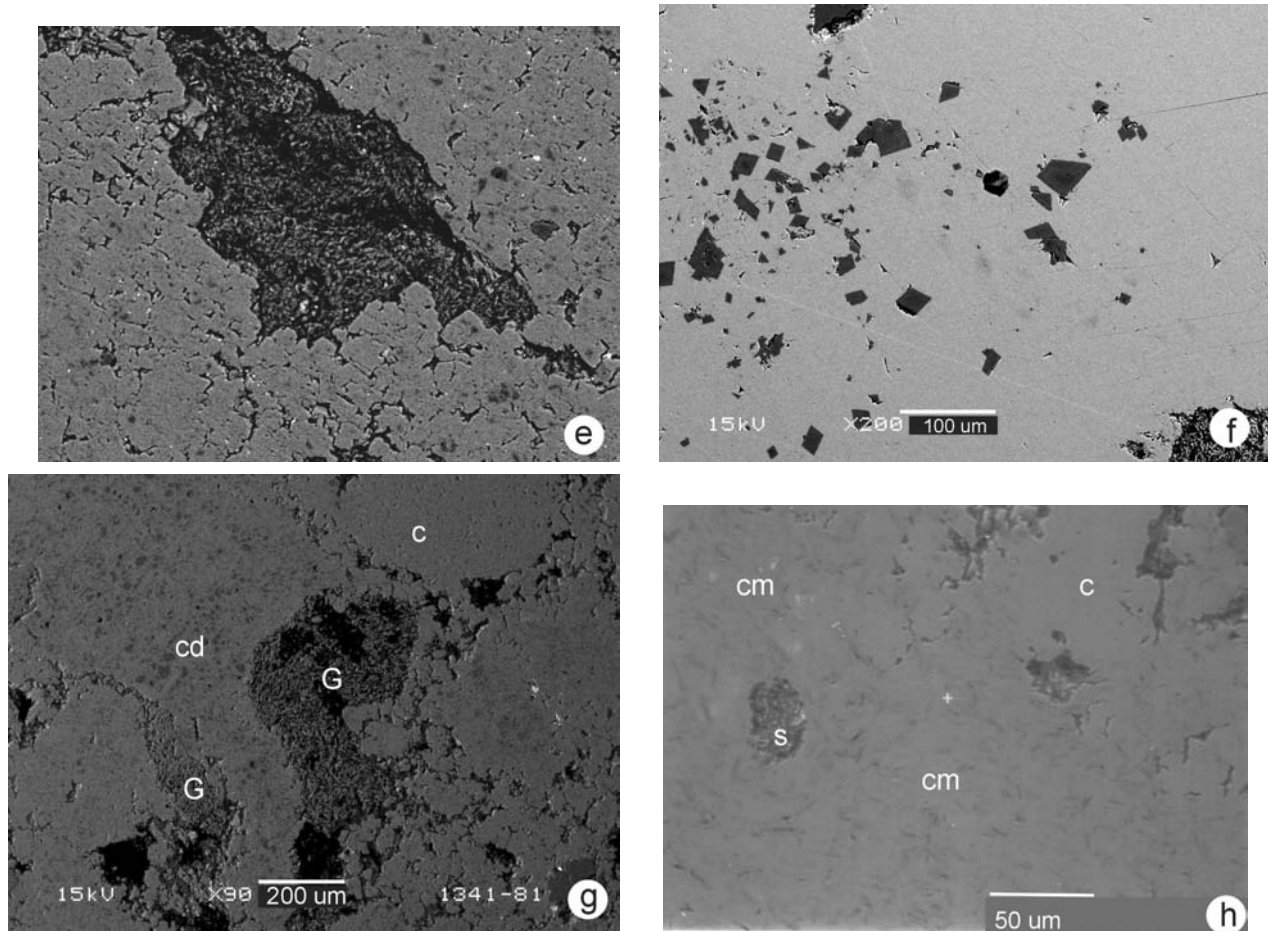


Fig. 7. *Continued.* Petrography of unit 6 at various scales: e) dark melt fragment completely altered to smectite in a recrystallized carbonate melt groundmass, sample Yax-1-892.32. The length of image is 290  $\mu\text{m}$ ; f) recrystallized carbonate melt consisting mainly of light-grey calcite and dark grey dolomite crystals. In lower right corner is a smectite-altered melt fragment. Groundmass of lower-most central part of thin section Yax-1-892-15 (c); g) carbonate and silicate melts. c = calcite melt, cd = calcite-dolomite melt. Note the tongue of this melt between the two silicate melt fragments (G). These silicate melts consist of plagioclase laths in a smectite mesostasis; h) carbonate melt fragment in upper left corner of image (d). A small part of the image is calcite melt (c) while the remainder is a microlite-bearing carbonate/silicate melt (see Geochemistry section). Note tiny smectite-altered silicate melt fragments (s).

7 well (U7 in Fig. 1), approximately 125 m of suevite at a depth of ~220–345 m are underlain by weakly shocked breccia. This low-shock breccia is derived mainly from the pre-impact platform rocks and in this aspect is similar to bunte breccia deposits at the Ries crater, Germany. The presence of thick suevite deposits at UNAM 5 and 7 outside the crater proper (unpublished study by B. Dressler, Mexico City 2001) and Y6 well within the crater (PEMEX company files) lead us to believe that a much thicker, possibly a few hundred meters thick suevite deposit originally existed at Yaxcopoil. It is unrealistic to assume that the suevite deposit between these three wells originally was only <30m thick. The Chicxulub impact occurred in a shallow marine environment. We believe that rapid erosion due to catastrophic backsurge of seawater after impact possibly led to erosion of much of the suevite. The Tertiary units from a depth of about 750 m downwards to the upper contact of the “redeposited” suevite at 795 m depth exhibit evidence for

turbulent depositional episodes and a rugged depositional environment; turbiditic units, and various conglomerates have been noted. Following the original, catastrophic erosional event, several episodes of erosion and redeposition may have been active over considerably long periods of time prior to final burial of the impact breccia by Tertiary sedimentary rocks. It is not unconceivable that these processes were active over many thousands of years. Therefore, the top of the redeposited suevite of unit 1 may not represent the K/T boundary. It, therefore, may also be futile to try to find any iridium anomaly associated with the uppermost allogenic breccia at Yax-1.

Units 3 and 4 beneath the suevite represent an intriguing sequence of rocks that, to our knowledge, has no known equivalence in any other terrestrial impact structure. As we have shown, the groundmass of unit 3 is very rich in tiny melt fragments, some of which are molded together. Silicate-carbonate melt clasts (Figs. 4c, 4d) and, in a few thin sections,

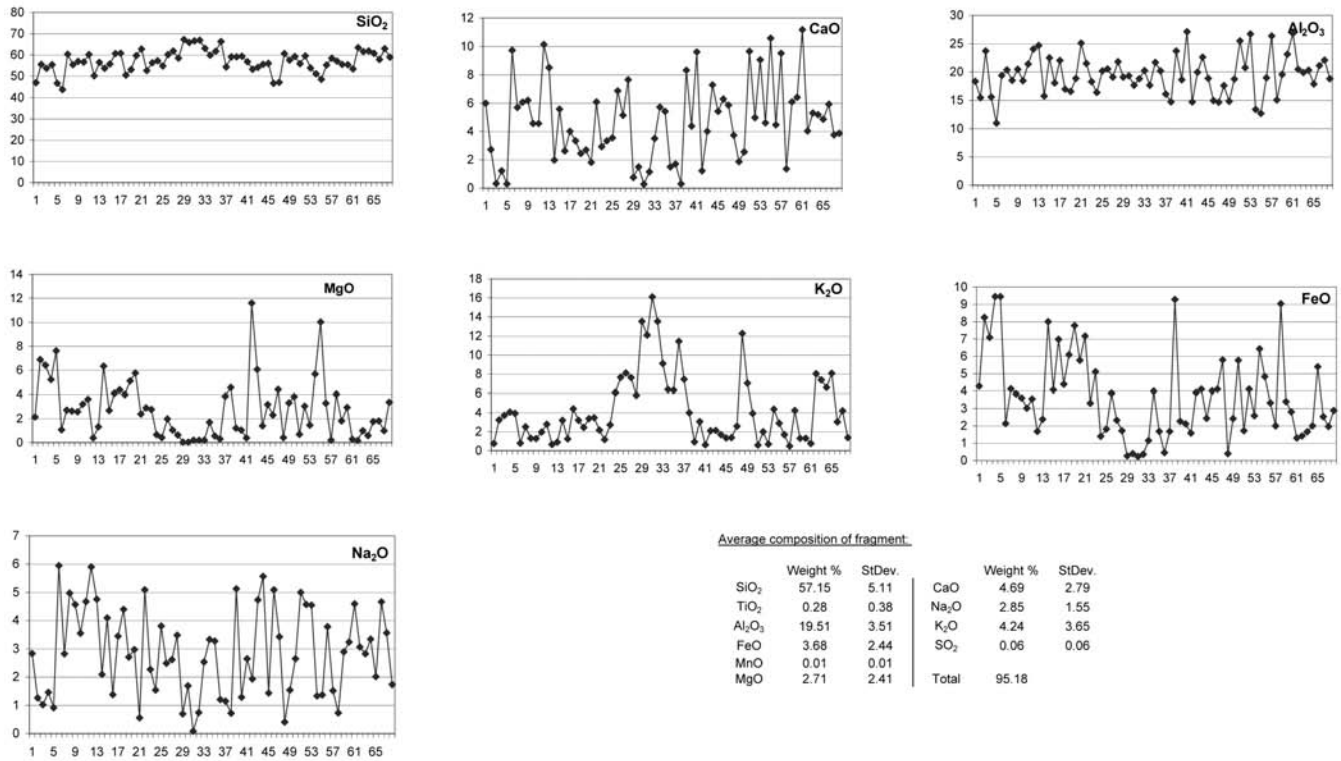


Fig. 8. Microprobe profile across laminated melt fragment in suevite (Yax-1 unit 2). Fragment is about 2.5 × 6 mm in size. Profile is across 2.5 mm width, perpendicular to lamination but only left border area of the clast was analyzed. Left probably represents smectite alteration, the center an alkali feldspar-rich zone, and the remainder a plagioclase/pyroxene composition. Sample Yax-1-819.65, clast B in Fig. 3b.

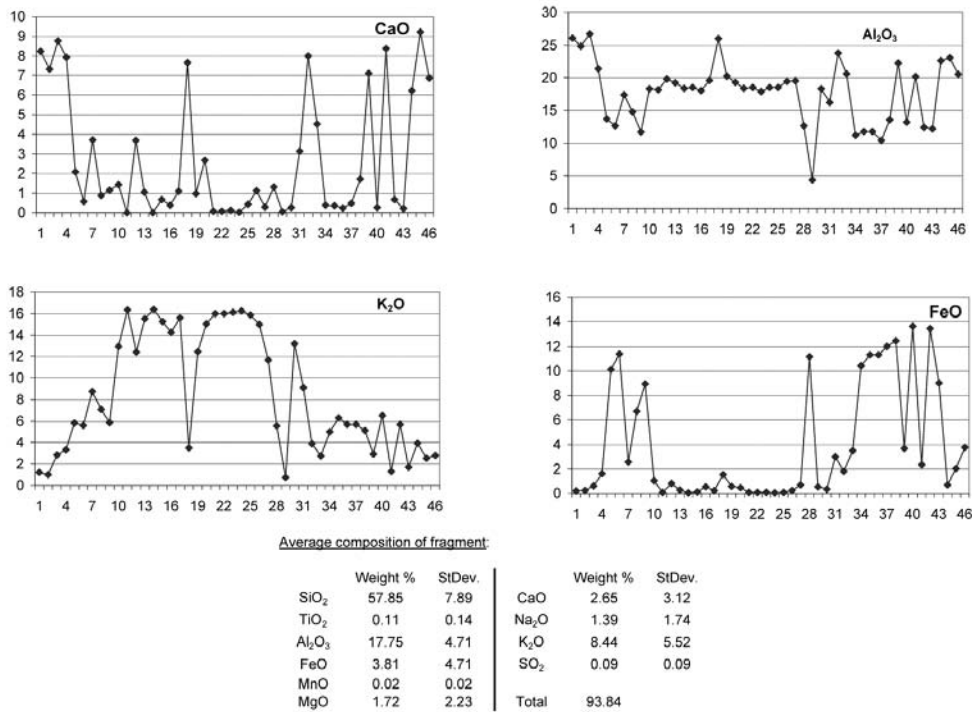


Fig. 9. Microprobe profile across laminated melt fragment in suevite (Yax-1 unit 2). The fragment is about 2 × 8 mm in size. Profile is across 2 mm width, perpendicular to lamination. From left to right: Andesitic composition, plagioclase/pyroxene compositions, wide zone of alkali feldspar composition zone of plagioclase/pyroxene compositions. Sample Yax-1-819.65, clast A in Fig. 3b.

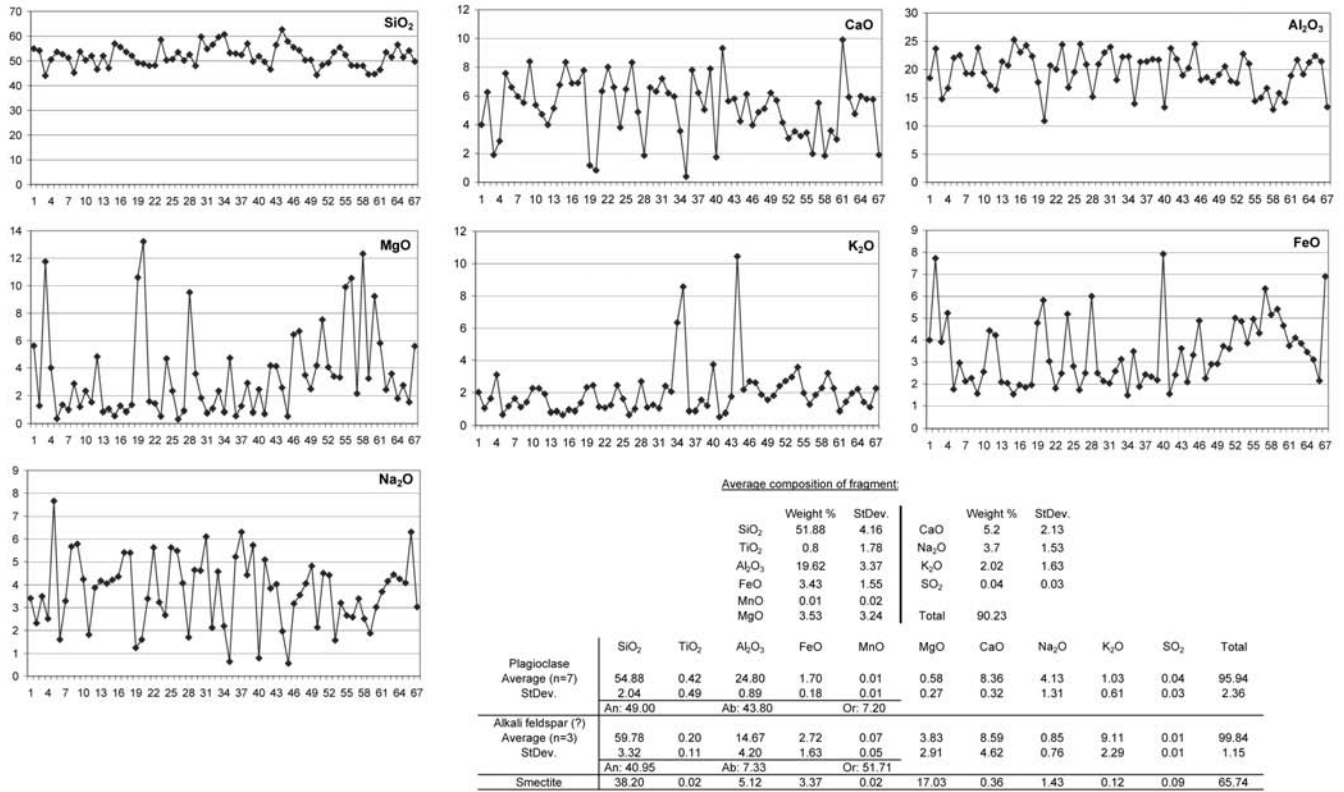


Fig. 10. Microprobe profile across melt fragment in sample Yax-1-826.25 in unit 3, average composition of melt fragment, and composition of mineral components. Profile is 0.57 mm long in a 10 × 25 mm size clast.

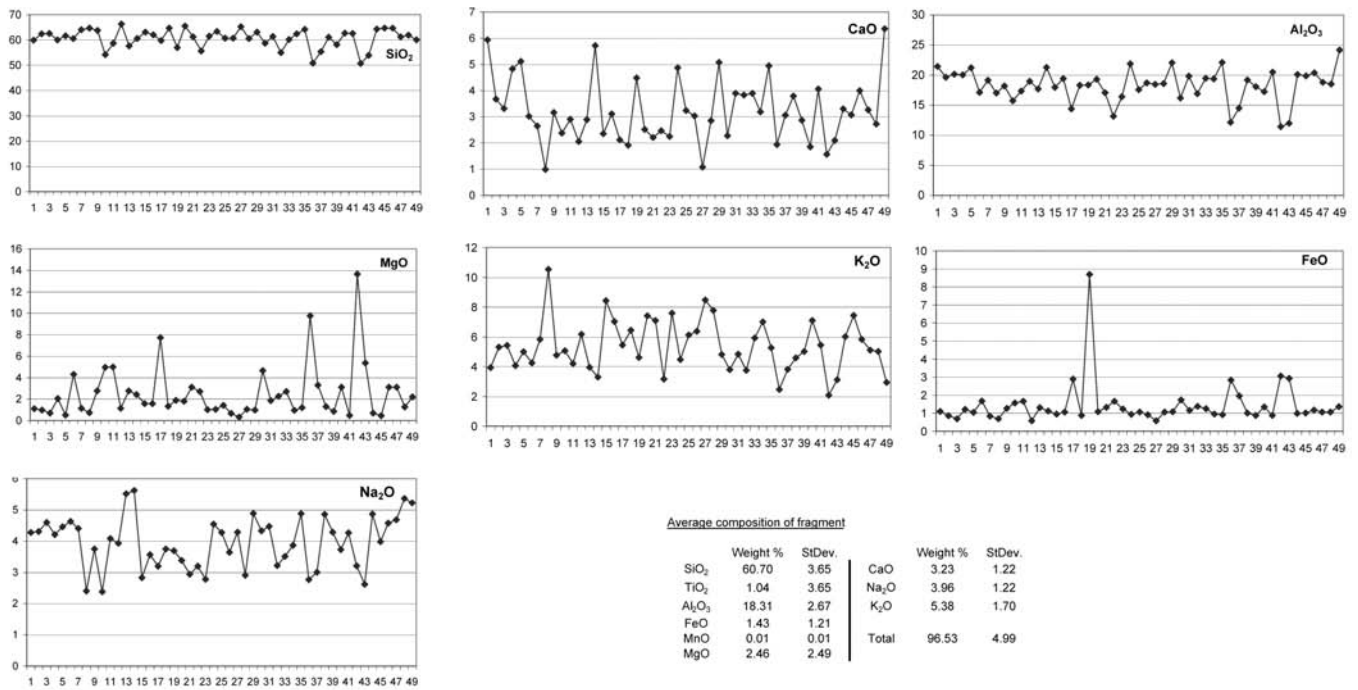


Fig. 11. Microprobe profile across silica-rich melt fragment in Yax-1-842.06, unit 3. Profile is 0.53 mm long.

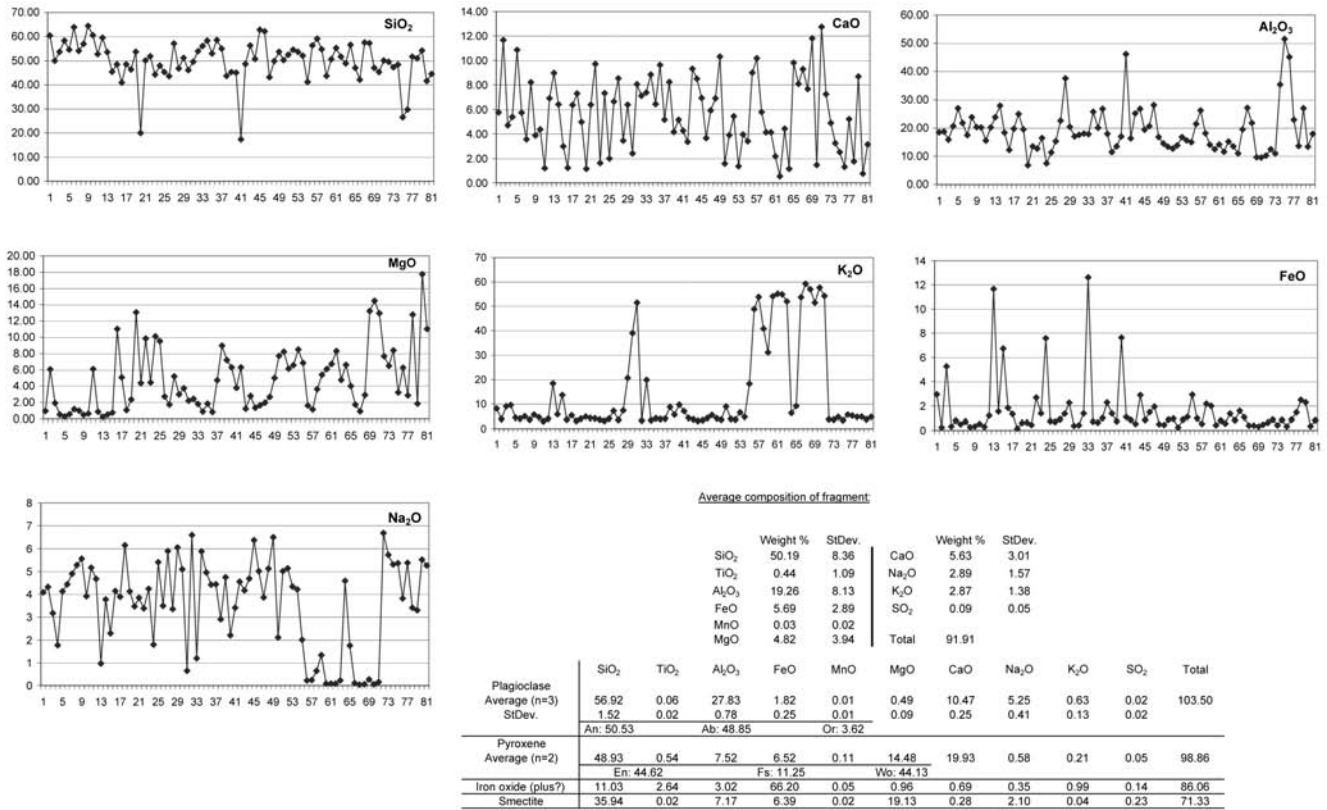


Fig. 12. Microprobe profile across melt rock fragment in sample Yax-1-852.02 (unit 4) and average composition of fragment and composition of plagioclase and pyroxene laths. Variation of alkali content content is indicative of a 16-point wide alkali feldspar-rich lamina. 0.6 mm long profile in a 6 × 10 mm size clast.

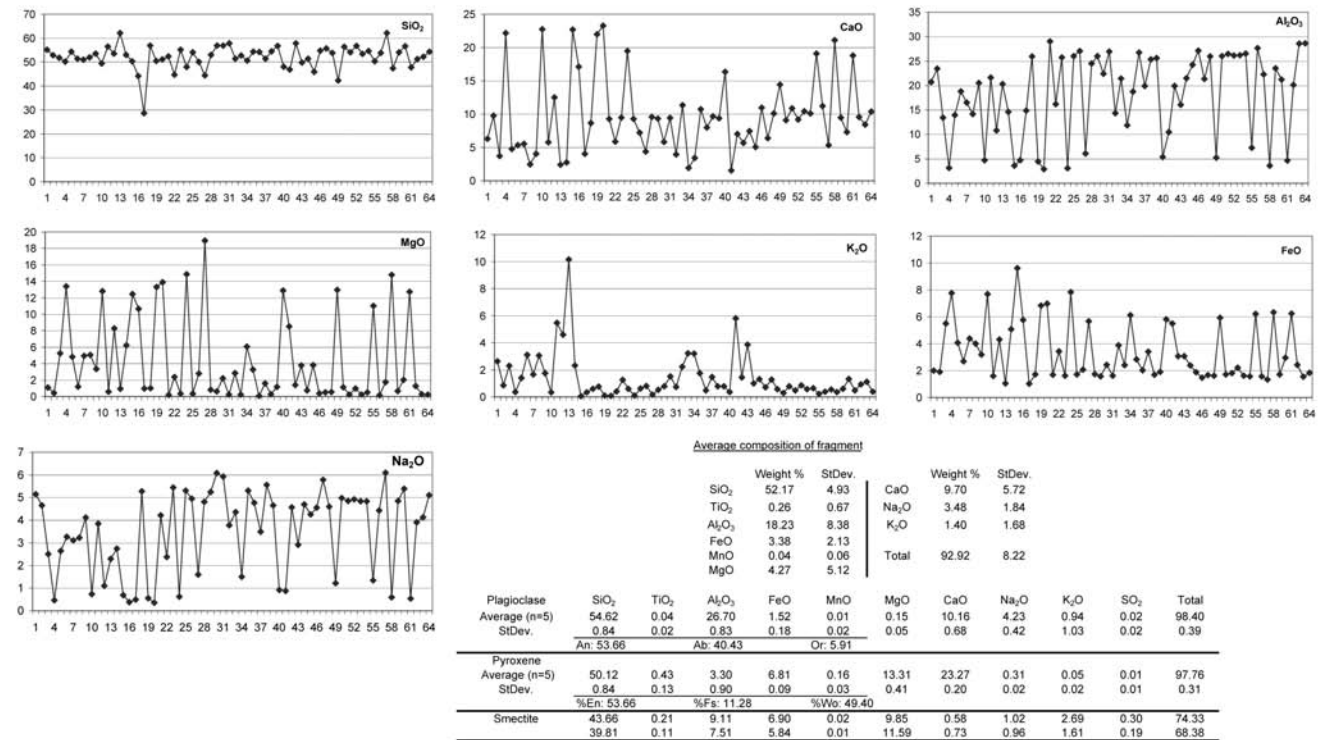


Fig. 13. Microprobe profile across melt rock fragment in sample Yax-1-862.05 (unit 5) and microlite compositions. Length of profile 0.72 mm.

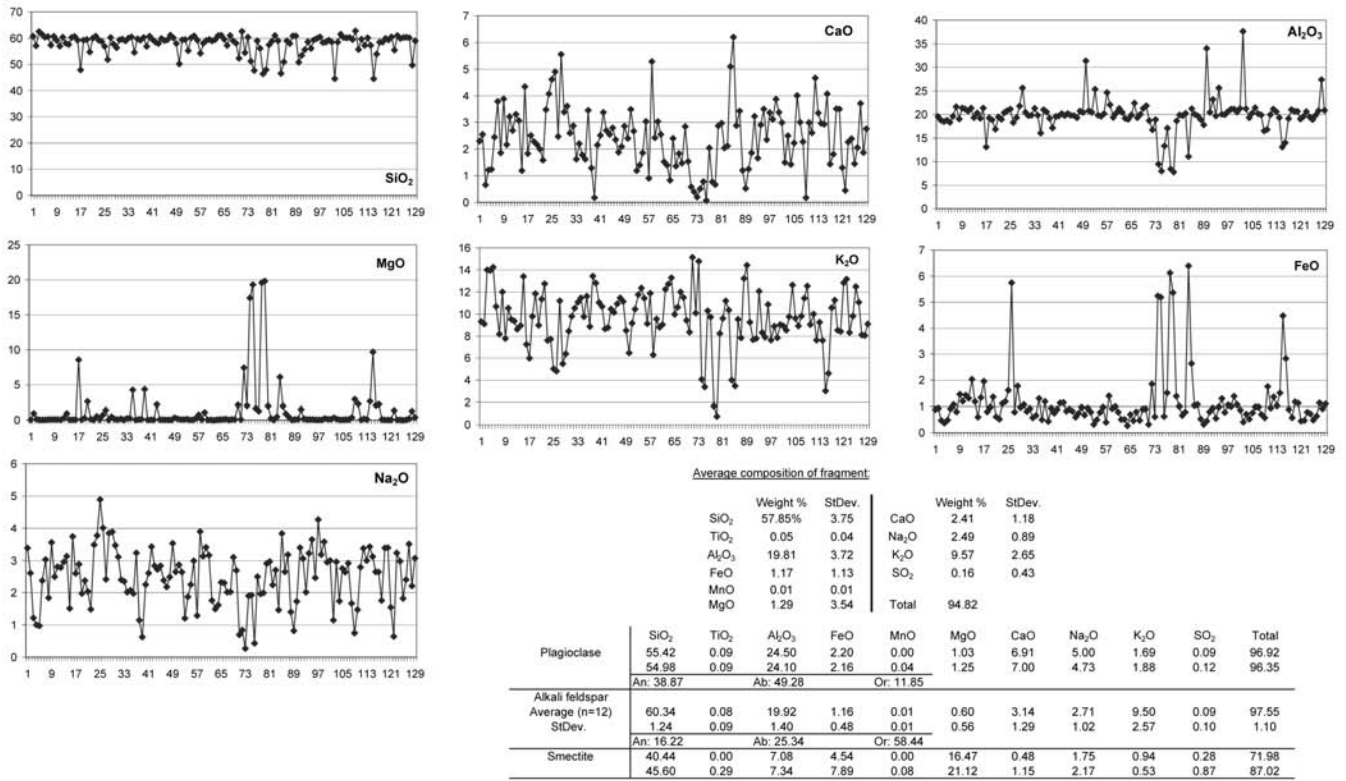


Fig. 14. Microprobe profile across melt fragment in Yax-1-891.27 (unit 6), average composition of fragment, and composition of microlite components. Fragment is 2.6 × 3.2 mm in size, profile 0.7 mm long.

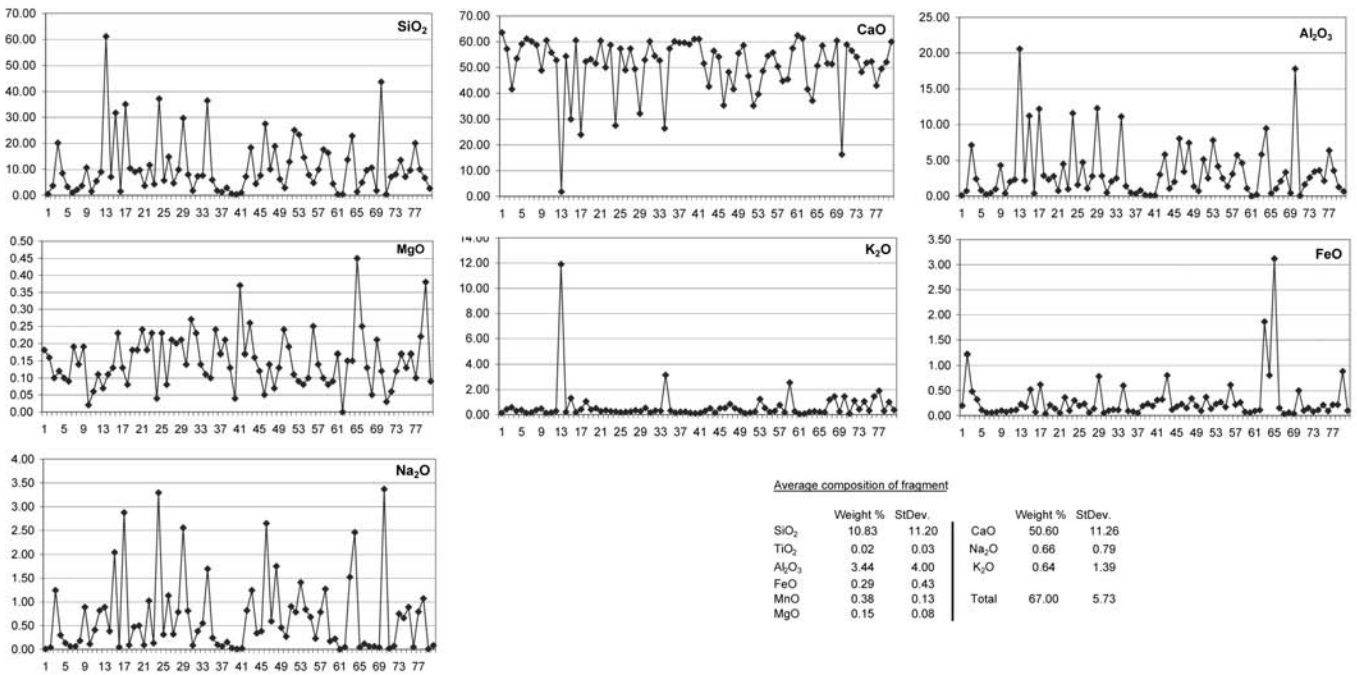


Fig. 15. Microprobe profile across siliceous carbonate melt fragment in sample Yax-1-885.70. Profile is 0.6 mm long. Note silica content of groundmass.

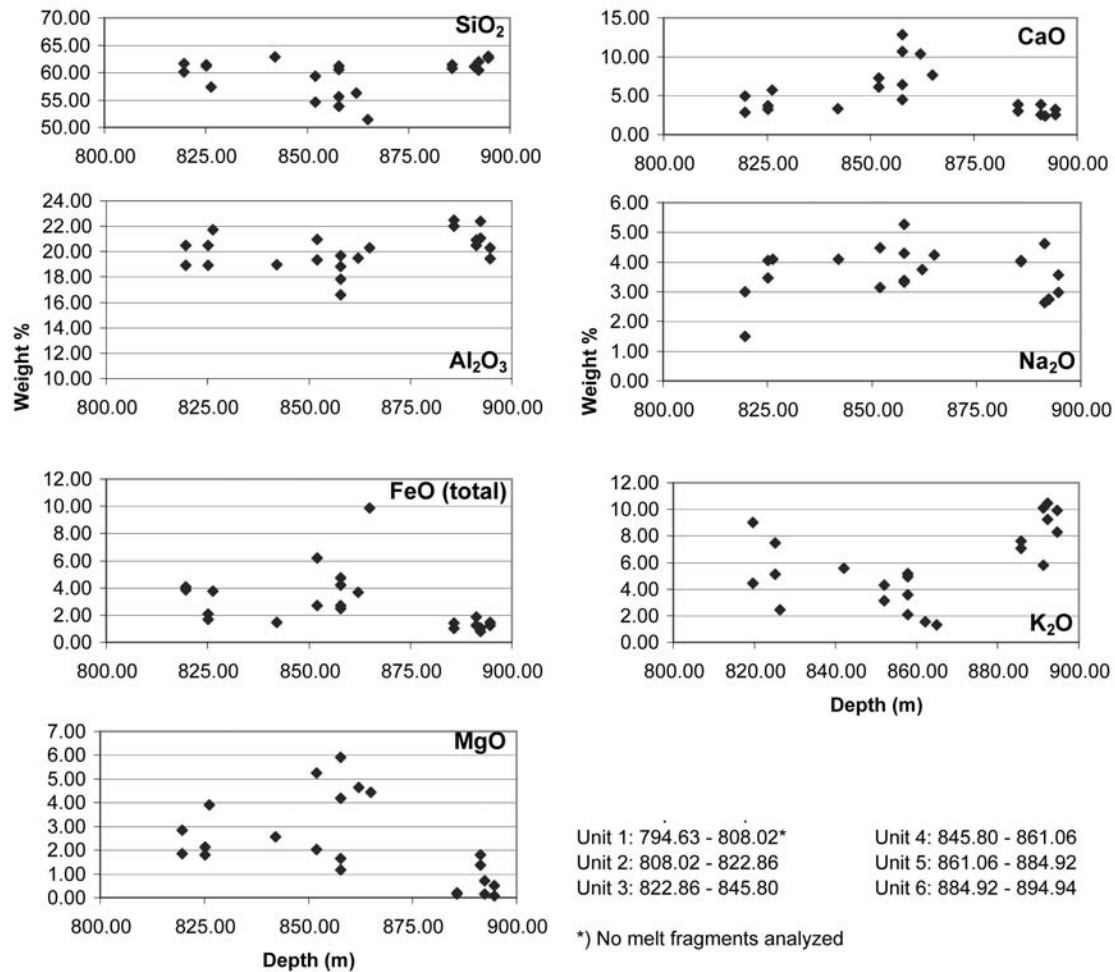


Fig. 16. Major oxides of melt fragments in Yax-1 impactites versus depth. Compare with Table 2.

a silicate/carbonate melt groundmass (Fig. 4h) have been noted. The schlieren-like shape of several large melt bodies (e.g. Fig. 4a) suggests that they were incorporated in the breccia while both breccia groundmass and melt had a consistency of a viscous melt. The 60–100  $\mu\text{m}$  chondrule-like bodies (Figs. 4f, 4g) in the groundmass should provide us with some good evidence on the processes responsible for brecciation and deposition of unit 3. Chondrules make up up to about 80% of some most common class of meteorites, the ordinary chondrites. The last word on their origin has not been written, but many researchers believe that some flash heating process probably melted stellar dust to form chondrules. In our context, it is noteworthy that D. Sears (University of Arkansas) envisions a chondrule forming process related to impact processes. He argues that chondrules formed on asteroids during an impact by a larger body (Symes et al. 1998). Our impact “chondrules” were not formed in zero gravity but in an equally turbulent, fiery cloud of rock and melt particles.

The groundmass of unit 4 is very similar to that of unit 3, however, it encloses many much larger fragments than unit 3.

Melt clasts commonly have contorted shapes (Fig. 5a). Some of them have outlines (Figs. 5c, 5d) that would not have survived in a clastic deposition process. They suggest corrosive absorption of the fragments by a high-temperature groundmass, a groundmass that, at least in places, apparently constituted a viscous carbonate-rich melt (Figs. 5d, 5e). All these observations lead us to believe that the breccias of unit 4 have an origin similar to that of unit 3 and that the two units actually were formed in one specific depositional process. The coexistence of clastic and melt groundmasses, the deposition in a high-temperature environment and the evidence of turbulent movement (“chondrules”) are similar to characteristics of glowing avalanches or pyroclastic flows in volcanic environments with a coarser base (unit 4) and a finer top (unit 3, nuée ardente), as described in many a textbook on volcanology. Corrosive action between hot fragments and hot groundmass apparently occurred after deposition.

Unit 5 is very different from any of the breccias that overlie it. It is rather homogeneous and, as we have shown, has the appearance of a flow breccia, similar to flow-top breccias of silica-rich volcanic extrusions. The groundmass

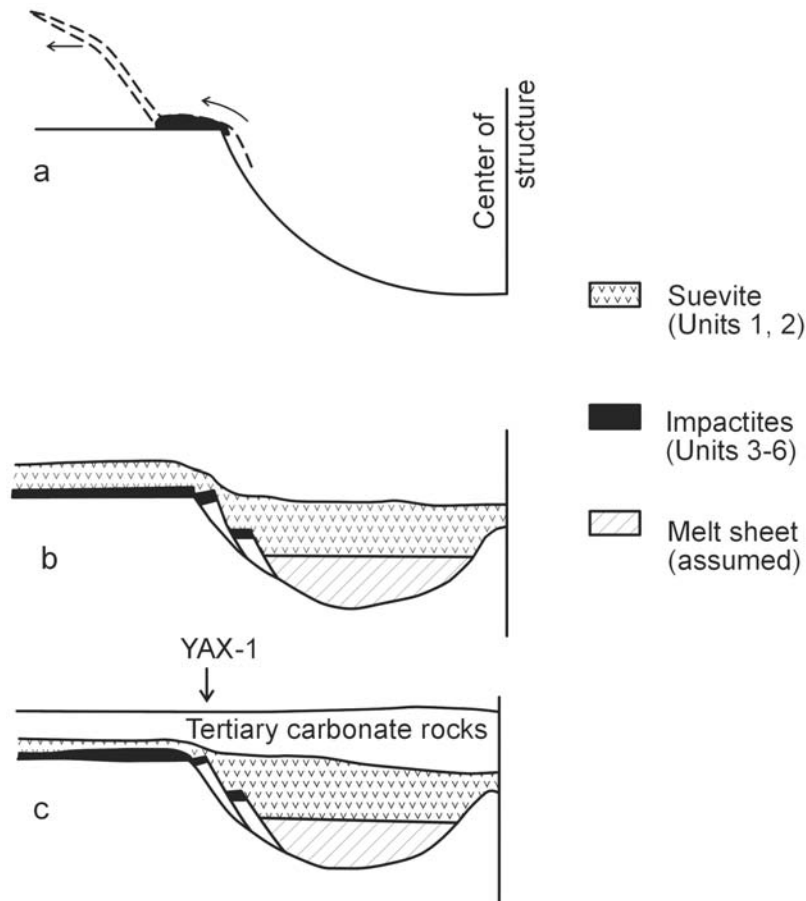


Fig. 17. Deposition of impact breccias and melts by ejecta curtain (units 3–6) at location Yaxcopoil and subsequent deposition, erosion and partial redeposition of fallback suevite (units 1–2): a) deposition of units 3–6 by ejecta curtain; b) emplacement of impact melt sheet and deposition of suevite; c) excavation crater wall collapse; d) partial erosion of suevite and redeposition/reworking of suevite before deposition of Tertiary cover rocks. Thickness of units are not to scale, however, note the reduced thickness of the suevite in (d) compared to (b) and (c). The redeposited unit 1 may very well contain material derived from “bunte breccia” type deposits from outside the crater cavity and not only locally derived suevitic material. Central uplift formation and ring formation are not shown.

between larger melt clasts is heterogeneous, but, in places, melt groundmass has been noted substantiating our comparison with flow breccias. Basement rock fragments in the melt breccia commonly show signs of incipient melts and as such fill the spaces between melt fragments.

The unit 6 breccia is very heterogeneous, again making proper fragment and matrix identification difficult. At least in the lower parts of unit 6, much of the groundmass is carbonate melt. It contains large target rock fragments, silicate melt fragments, and siliceous carbonate melt fragments (Figs. 7a–h). We have also noted evidence for welding of calcite melt with calcite/dolomite melt and silicate melt (Fig. 7g). Based on our core logging at the Yaxcopoil drill site and the study of about 10 thin sections of this unit under the light and electron microscopes, we interpret unit 6 as a melt breccia with some clastic material. The contact between units 5 and 6 is gradational and the two units may in some way represent an overturning of the target stratigraphy. Material from the upper target sequence (Cretaceous limestone and dolomite) forms

the lower part of the combined unit 5 and 6 breccia package, whereas unit 5 melts are derived from basement lithologies.

Our geochemical investigations, at present, do not provide us with much insight into the Yax-1 depositional environment. Overall, melt fragments are chemically rather homogeneous. Of the 24 melt fragments analyzed with the electron microscope, 16 fall in a 59 to 63 weight %  $\text{SiO}_2$  intermediate range, six are lower in  $\text{SiO}_2$  (51 to 57 weight %), and two are carbonate melts (Table 2). Melt fragments of unit 6 are potassium-rich, probably indicating post-depositional alteration. The more silica-poorer melts were probably derived from more mafic target rocks. We did not find any sulfur-rich melt rocks and anhydrite clasts in the Yax-1 breccias. Anhydrite clasts, however, have been noted by us in the breccias of UNAM 5, 6, and 7 cores. Therefore, the Yax-1 breccias are probably derived from a relatively restricted target area, possibly the excavation cavity close to Yaxcopoil. This interpretation, in our opinion, is substantiated by the differences of our geochemical results and those obtained by

Schuraytz et al. (1994) from the melt sheet within the excavation cavity. The melt rocks of wells C1 and Y6 have silica contents similar to those of most of the melt fragments analyzed by us.  $\text{Al}_2\text{O}_3$  and  $\text{K}_2\text{O}$ , however, are considerably lower. There are several additional differences (Table 2). Yax-1 melt fragments were probably derived from a more restricted target area in comparison to C1 and Y6 melts. The latter represent melting and mixing of a much larger target. The overall high potassium content of the Yax-1 samples is probably the result of alteration that did not affect the deep seated melt sheet at wells C1 and Y6. The absence of any anhydrite fragments in the Yax-1 impact breccias is further evidence that the impactite sequence between 795 and 895 m depth at Yaxcopoil represents a rather restricted source region.

We have stated above that the impact breccias of unit 3 to 6 have no known equivalents in any terrestrial impact structure. However, similar lithologies probably occur beneath the Tertiary cover rocks around the Chicxulub excavation cavity and, before erosion, may have existed around other impact craters. The closeness of Yaxcopoil to the rim of the excavation cavity, the unique petrography of Yax-1 breccias, led us to believe that these units represent some ground-surge deposit left behind by the ejecta curtain before deposition of the fallback suevite and its redeposition (units 1 and 2). Figure 17 depicts our model. The observation of truncated flow lamination at the border of many melt fragments is evidence for post depositional fragmentation of melt clasts that was probably caused by violent reaction of seawater with the superheated breccias, similar to phreomagmatic explosive activity in volcanic regimes. We are, however, aware that not all fragmentation of melt was caused by this process. It also occurred during ground-surge breccia emplacement. We are aware that our future investigations, and the studies by our colleagues also working on Yax-1 samples, will lead to refinement and possibly drastic changes to this model.

*Acknowledgments*—We are thankful to the staff of the microprobe and SEM laboratories of the Johnson Space Center, Houston, Texas, for their help and patience while B. Dressler was a visiting scientist at the Lunar and Planetary Institute, Houston. Thanks are also due to Dr. D. Black and Dr. S. Mackwell and staff of the Lunar and Planetary Institute for the generous support during the investigations that form the basis for this publication. We also thankfully acknowledge fruitful discussions with members of the Chicxulub working groups, especially Dr. W. U. Reimold, Dr. D. Stöffler, J. Smit, and M. Tuchscherer. We thank Dr. M. Harting, Dr. C. Koeberl, and an anonymous reviewer for their helpful reviews. The Lunar and Planetary Institute is operated by the University Research Association under contract with NASA. This is Lunar and Planetary Institute Contribution 1202.

*Editorial Handling*—Dr. Jaime Urrutia-Fucugauchi

## REFERENCES

- Brittan J., Morgan M., and Warner M. 1999. Near-surface seismic expression of the Chicxulub impact crater. In *Large meteorite impacts and planetary evolution*, edited by Dressler B. O. and Sharpton V. L. Geological Society of America Special Paper 339. pp. 269–279.
- Christeson G. L., Buffler R. T., and Nakamura Y. 1999. Upper crustal structure of the Chicxulub impact crater from wide-angle ocean bottom seismograph data. In *Large meteorite impacts and planetary evolution*, edited by Dressler B. O. and Sharpton V. L. Geological Society of America Special Paper 339. pp. 291–298.
- Dressler B. O. 1984. The effects of the Sudbury event and the intrusion of the Sudbury igneous complex on the footwall rocks of the Sudbury structure. In *The geology and mineral deposits of the Sudbury structure*, edited by Pye E. G., Naldrett A. L., and Giblin P. E. Special Volume 1. Toronto: Ontario Geological Survey. pp. 97–136.
- Dressler B. O., Sharpton V. L., Morgan J., Buffler R., Moran D., Smit J., Stöffler D., and Urrutia J. 2003. Investigating a 65-Ma-old smoking gun: Deep drilling of the Chicxulub impact structure. *EOS Transactions* 84:125–130.
- Dressler B. O. and Reimold W. U. Forthcoming. Order or chaos? Origin and mode of emplacement of breccias in floors of large impact structures. *Earth-Science Reviews*.
- Graup G. 1981. Terrestrial chondrules, glass spherules, and accretionary lapilli from suevite, Ries crater, Germany. *Earth Planetary Science Letters* 55:407–418.
- Grieve R. A. F., Stöffler D., and Deutsch A. 1991. The Sudbury structure: Controversial or misunderstood? *Journal of Geophysical Research* 96:22753–22764.
- Hildebrand A. R., Pilkington M., Connors M., Ortiz-Aleman C., and Chavez, R. E. 1995. Size and structure of the Chicxulub crater revealed by horizontal gravity gradients and cenotes. *Nature* 376: 415–417.
- Marin L. E., Urrutia-Fucugauchi J., Rebollo-Vieyra M., Soler-Arechalde A. M., and Sharpton V. L. 2000. *The Chicxulub Scientific Drilling Project: Strategy. ICDP Newsletter, vol. 2.*
- Morgan J. and Warner M. 1999. Morphology of the Chicxulub impact: Peak-ring crater or multi-ring Basin. In *Large meteorite impacts and planetary evolution*, edited by Dressler B. O. and Sharpton V. L. Geological Society of America Special Paper 339. pp. 281–290.
- Pouchou J. and Pichior F. 1991. Quantitative analysis of homogeneous or stratified microvolumes applying the model “PAP.” In *Electron probe quantification*, edited by Heinrich K. F. J., and Newbury D. E. New York: Plenum Press. pp. 31–75.
- Reimold W. U. and Gibson R. L. 1996. Geology and evolution of the Vredefort impact structure. *Journal African Earth Sciences* 23: 125–162.
- Sharpton V. L., Burke K., Camargo-Zanoguera A., Hall S. A., Lee D. S., Marin L. E., Suárez-Reynoso G., Quezada-Muñeton J. M., Spudis P. D., and Urrutia-Fucugauchi J. 1993. Chicxulub multiring impact basin: Size and other characteristics derived from gravity analysis. *Science* 261:1564–1567.
- Sharpton V. L., Marin L. E., Carney C., Lee S., Ryder G., Schuraytz B. C., Sikora P., and Spudis P. D. 1996. A model of the Chicxulub impact basin based on evaluation of geophysical data, well logs, and drill core samples. In *The Cretaceous-Tertiary event and other catastrophes in Earth history*, edited by Ryder G., Fastovsky D., and Schultz P. Geological Society of America Special Paper 307. pp. 55–74.
- Schuraytz B. C., Sharpton V. L., and Marin L. E. 1994. Petrology of impact-melt rocks at the Chicxulub multiring basin, Yucatán, Mexico. *Geology* 22:868–872.

- Symes S. J. K., Sears D. W. G., Taunton A., Akridge D. S., Huang S., Benoit P. H. 1998. The crystalline lunar spherules: Their formation and implications for the origin of meteoritic chondrules. *Meteoritics & Planetary Science* 33:13–29.
- Snyder D. B. and Hobbs R. W. 1999. Deep seismic reflection profiles across the Chicxulub crater. In *Large meteorite impacts and planetary evolution*, edited by Dressler B. O. and Sharpton V. L. Geological Society of America Special Paper 339. pp. 263–268.
- Urrutia Fucugauchi J., Morán Zenteno D., Sharpton V. L., Buffler R., Stöffler D., and Smit J. 2001. *The Chicxulub scientific drilling project. Infraestructura científica y desarrollo tecnológico 3*. Mexico City: Insitute de Geofísica, Universidad Nacional Autónoma de Mexico. 45 p.

#### APPENDIX-METHODS OF INVESTIGATION

Electron microscopy was accomplished using a JEOL 5910LV scanning electron microscope with integrated IXRF Systems energy dispersive X-ray detector. Backscattered electron images were collected using an accelerating voltage of 15 kV. Qualitative phase identification was conducted with this instrumentation. Subsequently, quantitative chemical analysis was conducted using a Cameca SX100 scanning electron microprobe with five wavelength dispersive X-ray spectrometers and an IXRF Systems energy dispersive X-ray

detector. The analyses were collected using beam conditions of 15 kV, 20 nA, and counting times of 20 seconds per peak per element. The counting statistics for each element collected on natural mineral standards had standard deviations of less than one percent. The compositional determinations were calculated by processing the analyses with the PAP procedures of Pouchou and Pichior (1991), assuming stoichiometric formulae. Some of the analyses have low totals because they do not meet these criteria at the sub-micrometer scale due to averaging of mixed phases, impact damage and alteration.

---